Journal of Medicinal Chemistry

Article

Design of 4-oxo-1-aryl-1,4-dihydroquinoline-3-carboxamides as selective negative allosteric modulators of metabotropic glutamate receptor subtype 2

Andrew S Felts, Alice L Rodriguez, Katrina A Smith, Julie L. Engers, Ryan D. Morrison, Frank W. Byers, Anna L. Blobaum, Charles W. Locuson, Sichen Chang, Daryl F. Venable, Colleen M Niswender, J. Scott Daniels, P. Jeffrey Conn, Craig W Lindsley, and Kyle A Emmitte

J. Med. Chem., **Just Accepted Manuscript** • DOI: 10.1021/acs.jmedchem.5b01371 • Publication Date (Web): 02 Nov 2015

Design of 4-oxo-1-aryl-1,4-dihydroquinoline-3-carboxamides as selective negative allosteric modulators of metabotropic glutamate receptor subtype 2

Andrew S. Felts,[†] Alice L. Rodriguez,[†] Katrina A. Smith,[†] Julie L. Engers,[†] Ryan D. Morrison,[†,∥] Frank W. Byers,[†] Anna L. Blobaum,[†] Charles W. Locuson,[†,§] Sichen Chang,[†] Daryl F. Venable,[†,⊥] Colleen M. Niswender,[†] J. Scott Daniels,[†,∥] P. Jeffrey Conn,[†] Craig W. Lindsley,[†,‡] and Kyle A. Emmitte*[,†,‡,#]

[†]Vanderbilt Center for Neuroscience Drug Discovery, Department of Pharmacology, Vanderbilt University Medical Center, Nashville, Tennessee 37232

[‡]Department of Chemistry, Vanderbilt University, Nashville, TN 37232

KEYWORDS. Metabotropic glutamate receptor subtype 2 ($mGlu_2$), negative allosteric modulator (NAM), major depressive disorder (MDD), treatment-resistant depression (TRD), Alzheimer's disease

ABSTRACT. Both orthosteric and allosteric antagonists of the group II metabotropic glutamate receptors (mGlus) have been used to establish a link between $mGlu_{2/3}$ inhibition and a variety of CNS diseases and disorders. Though these tools typically have good selectivity for $mGlu_{2/3}$

versus the remaining six members of the mGlu family, compounds that are selective for only one of the individual group II mGlus have proved elusive. Herein we report on the discovery of a potent and highly selective $mGlu_2$ negative allosteric modulator **58** (VU6001192) from a series of 4-oxo-1-aryl-1,4-dihydroquinoline-3-carboxamides. The concept for the design of this series centered on morphing a quinoline series recently disclosed in the patent literature into a chemotype previously used for the preparation of muscarinic acetylcholine receptor subtype 1 positive allosteric modulators. Compound **58** exhibits a favorable profile and will be a useful tool for understanding the biological implications of selective inhibition of $mGlu_2$ in the CNS.

INTRODUCTION

Glutamate (L-glutamic acid) is the major excitatory neurotransmitter in the mammalian central nervous system (CNS) and exerts its effects through both ionotropic and metabotropic glutamate receptors (mGlus). The mGlus belong to family C of the G-protein-coupled receptors (GPCRs) and are characterized by a seven transmembrane (7TM) α-helical domain connected via a cysteine rich-region to a large bi-lobed extracellular amino-terminal domain. The orthosteric binding site is found within this amino-terminal domain for each of the eight members of the mGlu family. The mGlus are further categorized into three groups according to their homology, preferred signal transduction mechanisms, and pharmacology. The group I mGlus ($mGlu_1$ and $mGlu_5$) are primarily located post-synaptically in neurons and coupled via G_q to the activation of phospholipase C, which leads to the elevation of intracellular calcium and activation of protein kinase C (PKC). On the other hand, group II mGlus ($mGlu_2$ and $mGlu_3$) and group III mGlus ($mGlu_4$, $mGlu_6$, $mGlu_7$ and $mGlu_8$) are primarily located pre-synaptically and are coupled via $G_{i/o}$ to the inhibition of adenylyl cyclase activity.[1-3] The expression of the group

II mGlus is wide throughout the CNS; moreover, both are found in brain regions associated with emotional states such as the amygdala, hippocampus, and prefrontal cortex.[4,5]

With multiple compounds having advanced into clinical trials in schizophrenic patients, the design of selective and drug-like positive allosteric modulators (PAMs) of $mGlu_2$ is significantly more advanced than complementary research directed toward selective negative allosteric modulators (NAMs) of the same receptor.[6] Still, the literature contains multiple examples of highly optimized orthosteric antagonists and NAMs of the group II mGlus. Though these compounds typically possess good levels of selectivity against the other members of the mGlu family, they lack appreciable selectivity between $mGlu_2$ and $mGlu_3$.[7] Consequently, much has been learned regarding the potential utility of group II mGlu inhibition through the use of these tools in animal models of various CNS disorders. The bulk of such studies have employed the two orthosteric antagonists **1** (LY341495)[8] and **2** (MGS0039)[9] (Figure 1). Specifically, potential therapeutic applications of group II mGlu antagonists have been established in obsessive-compulsive disorder (OCD),[10,11] anxiety,[12] cognition,[13] and Alzheimer's disease.[14–16] Additionally, substantial work with these compounds has been directed toward establishing a role for $mGlu_{2/3}$ antagonists as novel antidepressants.[9,10,12,17–22] Perhaps most intriguing are studies demonstrating efficacy in animal models of treatment-resistant depression (TRD)[23] and anhedonia.[24]

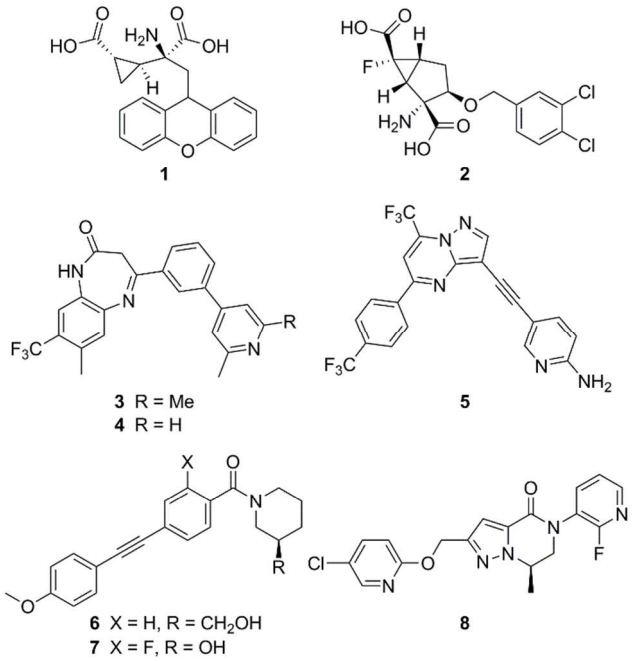

Figure 1. $mGlu_{2/3}$ orthosteric antagonist tools **1** and **2**, $mGlu_{2/3}$ NAM tools **3** and **4**, Roche $mGlu_{2/3}$ NAM clinical compound **5**, first-generation selective $mGlu_3$ NAMs **6** and **7**, and $mGlu_3$ NAM *in vivo* tool **8**.

Reports of *in vivo* studies with $mGlu_{2/3}$ NAMs are less prevalent; yet, two related compounds from a series of 4-aryl-1,3-dihydro-2*H*-benzo[*b*][1,4]diazepin-2-ones, **3** (RO4491533)[25] and **4** (RO4432717)[26,27] (Figure 1), are worth noting. Studies in rodent models of depression[25,28] and cognition[27,29,30] with these tools have been disclosed and show similar results as those observed with $mGlu_{2/3}$ orthosteric antagonists. Additionally, another structurally distinct $mGlu_{2/3}$ NAM, **5** (decoglurant, RO4995819)[31] from Roche (Figure 1), advanced into a phase II trial in patients with major depressive disorder (MDD) (NCT01457677).[32] Thus, the evidence for a therapeutic application with $mGlu_{2/3}$ antagonists is compelling; however, further elucidation is required regarding the individual importance of $mGlu_2$ and $mGlu_3$ in these various disorders. As such, we have been pursuing the design of selective antagonists of each receptor for use as *in vivo* tools.

Our initial success came in the design of selective $mGlu_3$ NAMs from a series of 1,2-diphenylethyne compounds represented by tool compounds **6** (VU0463597, ML289)[33] and **7** (VU0469942, ML337)[34,35] (Figure 1). More recently we reported on another $mGlu_3$ NAM, **8** (VU0650786),[36] that is a superior *in vivo* tool and has demonstrated efficacy in rodent models of anxiety/OCD and depression.[36] Having selective $mGlu_3$ NAMs from multiple chemotypes in hand, we sought strategies for the design of selective $mGlu_2$ NAMs for the purpose of thoroughly evaluating the therapeutic potential of each individual target. Our first successful execution of such a strategy is described in this manuscript.

RESULTS AND DISCUSSION

Scaffold Design. In our search for new scaffolds suitable for the design of selective $mGlu_2$ NAMs, we were intrigued by a set of quinoline-2-carboxamide compounds **9** developed at Merck and disclosed in the patent literature (Figure 2).[7,37] A survey of the functional $mGlu_2$ NAM activity presented in this application showed substantial tolerance for functional diversity at the 7-position with a variety of linkers connected to a number of unsaturated and saturated ring systems (**A**). The 4-position demonstrated a preference for aryl and heteroaryl rings (**B**), and a primary amide was preferred over a nitrile at the 2-position. We prepared an exemplar compound **10** and tested it in our own cell-based functional assays for $mGlu_2$ and $mGlu_3$.[35] These fluorescence-based assays measure calcium mobilization induced by receptor activation in a cell line stably expressing either rat $mGlu_2$ or rat $mGlu_3$ along with the promiscuous G-protein $G_{\alpha 15}$ and are capable of detecting agonists, PAMs, and NAMs. Compound **10** exhibited potent NAM activity at $mGlu_2$ and no evidence of $mGlu_3$ activity up to the highest concentration tested (30 μM). The quinoline-2-carboxamide $mGlu_2$ NAMs were reminiscent of another series of allosteric

modulators developed at Merck, the 4-oxo-1,4-dihydroquinoline-3-carboxylic acid muscarinic acetylcholine receptor subtype 1 (M_1) PAMs **11**.[38–40] Our hypothesis was that a new $mGlu_2$ NAM scaffold **12** might be obtained within a 4-oxo-1,4-dihydroquinoline series by appending appropriately linked groups (**A**) at the 6-position and installing *N*-aryl rings (**B**) at the 1-position in the context of a primary amide at the 3-position. In addition, the extensive M_1 PAM SAR already developed in this chemotype indicated that such changes would not be favorable for that target.

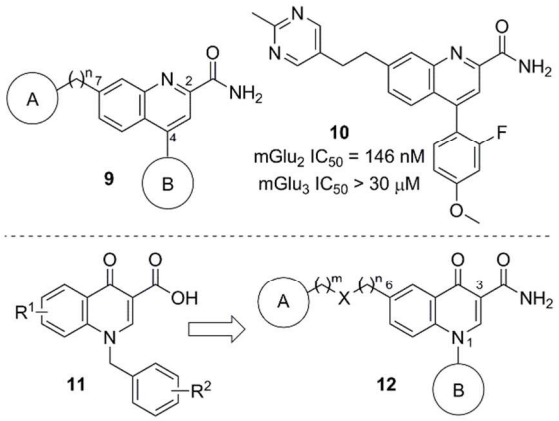

Figure 2. Merck quinoline-2-carboxamide $mGlu_2$ NAM scaffold **9** and representative compound **10**; Merck 4-oxo-1,4-dihydroquinoline-3-carboxylic acid M_1 PAM scaffold **11**; Proposed 4-oxo-1-aryl-1,4-dihydroquinoline-3-carboxamide $mGlu_2$ NAM scaffold **12**.

Synthesis of Compounds. It was envisioned that a number of interesting analogs could be prepared from versatile 6-bromo intermediate **15** (Scheme 1). The synthesis began with commercially available acid **13**. Treatment of **13** with two equivalents of butyl lithium followed by addition of 5-bromo-2-fluoro-benzoyl chloride provided β-ketoester **14**. Reaction of **14** with *N,N*-dimethylformamide dimethyl acetal followed by a suitable aryl amine under microwave

heating afforded the desired intermediate **15**. Compound **15** could be converted to primary amide **16** through heating in ammonia in methanol under microwave irradiation to give **16**. Where possible, **16** was used as a common intermediate; however, certain transformations proved incompatible with the primary amide functional group and necessitated the use of ester **15** with subsequent conversion to the primary amide at a later stage. Reaction of **16** with commercially available aryl alcohols (R^1OH) in the presence of copper (I) iodide and dimethylglycine provided aryl ether analogs **17**–**19** (Table 1). For synthesis of ethers **23**–**29** (Table 1), conversion of bromide **15** to alcohol **20** was accomplished with a palladium catalyzed hydroxylation.[41] Acid **20** was converted to methyl ester **21** via a Fischer esterification. A Mitsunobu coupling[42] with commercial alcohols (R^2OH) was employed for installation of the various 6-substituted ethers to afford **22**. Conversion of the ester moieties to the corresponding primary amides to yield **23**–**29** was carried out as described previously. Finally, the synthesis of amine analogs **31**–**42** (Table 2) was accomplished by first reacting bromide **15** with commercially available amines in a Buchwald-Hartwig amination reaction[43] to yield **30**. Conversion of **30** to analogs **31**–**42** was carried out as described previously.

Scheme 1. Synthesis of 6-heteroatom linked analogs[a]

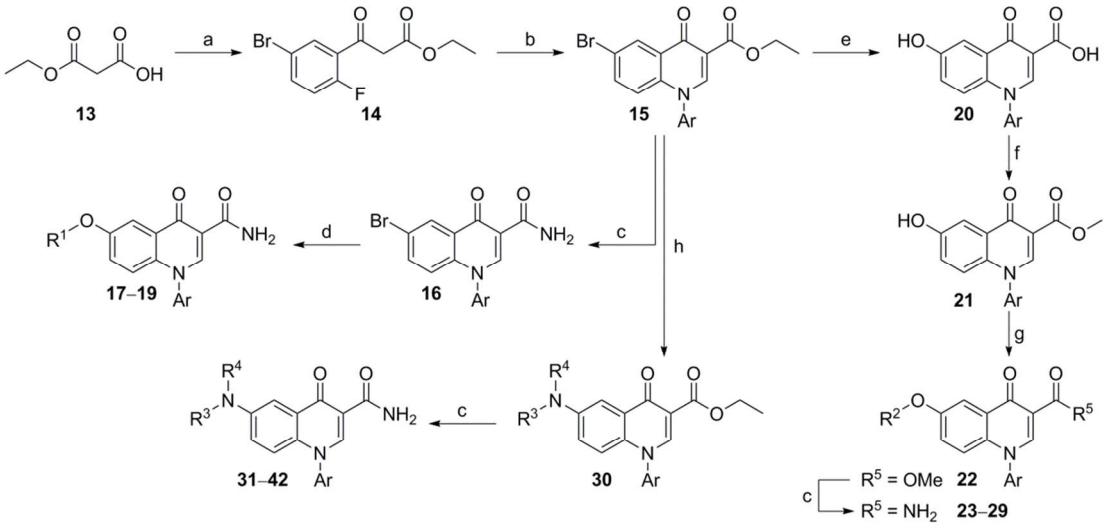

[a] Reagents and conditions: (a) *n*-BuLi, 2,2'-bipyridyl, –30 ºC to –5 ºC, then 5-bromo-2-fluoro-benzoyl chloride, –78 ºC to –30 ºC, 67%; (b) *N,N*-dimethylformamide dimethyl acetal, DMF, microwave, 120 ºC, 15 min, then $ArNH_2$, microwave, 150 ºC, 20 min, 60–98%; (c) 7N NH_3 in MeOH, microwave, 150 ºC, 60 min, 29–99%; (d) R^1OH, CuI, Cs_2CO_3, $Me_2NCH_2CO_2H$, microwave, 150 ºC, 15 min, 26–56% (e) KOH, $Pd_2(dba)_3$, *t*-BuXphos, dioxane, H_2O, microwave, 150 ºC, 15 min, 99%; (f) MeOH, con. H_2SO_4, reflux, 74%; (g) R^2OH, PPh_3, D^tBAD, THF, 40–98%; (h) HNR^3R^4, $Pd_2(dba)_3$, Xantphos, Cs_2CO_3, PhMe, 110 ºC, 8–54%.

In addition to the 6-heteroatom linked analogs, 6-carbon linked compounds were prepared from intermediates **15** and **16** (Scheme 2). Methylene-linked tertiary amine analogs **45–66** (Tables 3 and 4) were accessed through bromide **16**, which was first converted to vinyl intermediate **43** via a Suzuki coupling with potassium vinyltrifluoroborate.[44] Dihydroxylation of the olefin and subsequent *in situ* periodate cleavage of the resultant diol gave aldehyde **44**. Analogs **45–66** were then prepared through reductive aminations with **44** and commercially available secondary amines (HNR^2R^3). For preparation of methyleneoxy linked analogs **70–78** (Table 5), bromide **15** was converted to aldehyde **67** via an analogous vinylation,

dihydroxylation, and periodate cleavage as described above. Sodium borohydride reduction of **67** gave primary alcohol **68**, which was reacted in a Mitsunobu coupling[42] with commercial alcohols (R^4OH) to give ether intermediate **69**. Conversion of the ester moieties to the corresponding primary amides to yield **70–78** was carried out as described previously. Ethylene linked analogs **81–91** (Table 6 and Table 7) were also prepared from bromide **15** through initial preparation of alkynes **79**. Two methods were employed for preparation of these alkyne intermediates **79**, each relying on Sonogashira couplings[45] with bromide **15**. A coupling with **15** and a terminal alkyne (R^6CCH) gave **79** directly. Alternatively, a coupling with trimethylsilylacetylene followed by fluoride mediated silyl cleavage gave a 6-alkyne intermediate that was coupled to an aryl bromide (R^6Br) to afford **79**. A palladium catalyzed hydrogenation of the alkyne moiety provided **80**, which was reacted with ammonia as described previously to yield the target compounds **81–91**.

Scheme 2. Synthesis of 6-carbon linked analogs[a]

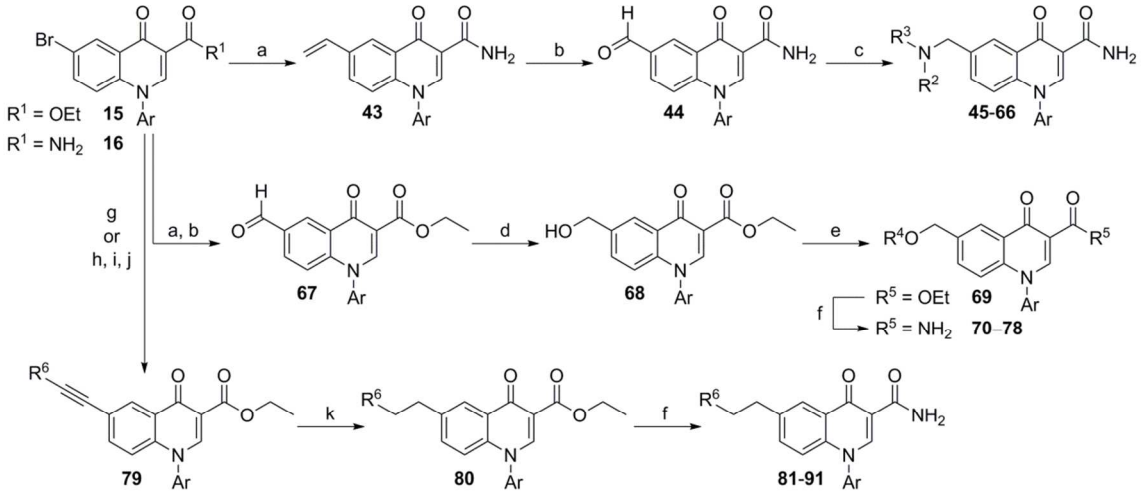

[a] Reagents and conditions: (a) H_2CCHBF_3K, $Pd(dppf)\cdot CH_2Cl_2$, NEt_3, *n*-propanol, 100 ºC, 75–100%; (b) OsO_4, NMO, acetone, H_2O, then $NaIO_4$, 91–99%; (c) HNR^2R^3, $NaBH(OAc)_3$, AcOH,

CH_2Cl_2, 7–81%; (d) $NaBH_4$, EtOH, 0 ºC, 36–57%; (e) R^4OH, PPh_3, D^tBAD, THF, 14–98%; (f) 7N NH_3 in MeOH, microwave, 150 ºC, 15 min, 10–94%; (g) R^6CCH, $PdCl_2(PPh_3)_2$, CuI, NEt_3, DMF, microwave, 150 ºC, 15 min, 23–54%; (h) Me_3SiCCH, $PdCl_2(PPh_3)_2$, CuI, NEt_3, DMF, microwave, 150 ºC, 15 min, 83%; (i) TBAF, THF, 70%; (j) R^6Br, $PdCl_2(PPh_3)_2$, CuI, NEt_3, DMF, microwave, 150 ºC, 15 min, 21–47%; (k) 10% Pd/C, MeOH, H_2 (1 atm), 63–99%.

In the case of the aforementioned 4-oxo-1,4-dihydroquinoline-3-carboxylic acid M_1 PAM scaffold, Merck has also shown that a 4*H*-quinolizin-4-one functioned as an effective bioisostere for the core of the chemotype.[46–48] As such, we decided to prepare analogs with this core to evaluate its potential as an $mGlu_2$ NAM scaffold as well (Scheme 3). The synthesis began with lithiation of 5-hydroxy-2-methylpyridine and subsequent *in situ* reaction with commercially available diethyl 2-(ethoxymethylene)malonate **92** to give 7-hydroxy-4-oxo-4*H*-quinolizine **93**. The alcohol was protected as its methoxymethyl ether **94**, which was then selectively brominated at the 1-position to afford **95**. A Suzuki coupling with 4-fluorophenylboronic acid provided intermediate **96**. Acidic cleavage of the protecting group and simple filtration of the precipitated product gave **97**, which served as the key intermediate for the synthesis of analogs. Ether compounds **99–102** (Table 8) were prepared via Mitsunobu coupling[42] with commercial alcohols (R^1OH) to yield **98**, which was converted to primary amides **99–102** as described above. Intermediate **97** was also converted to the corresponding triflate **103**, which was subjected to an analogous vinylation, dihydroxylation, and periodate cleavage as described previously to afford aldehyde **104**. Finally, conversion of **104** to amines **105** and ultimately final compounds **106–108** followed methods outlined herein above.

Scheme 3. Synthesis of 4*H*-quinolizin-4-one analogs[a]

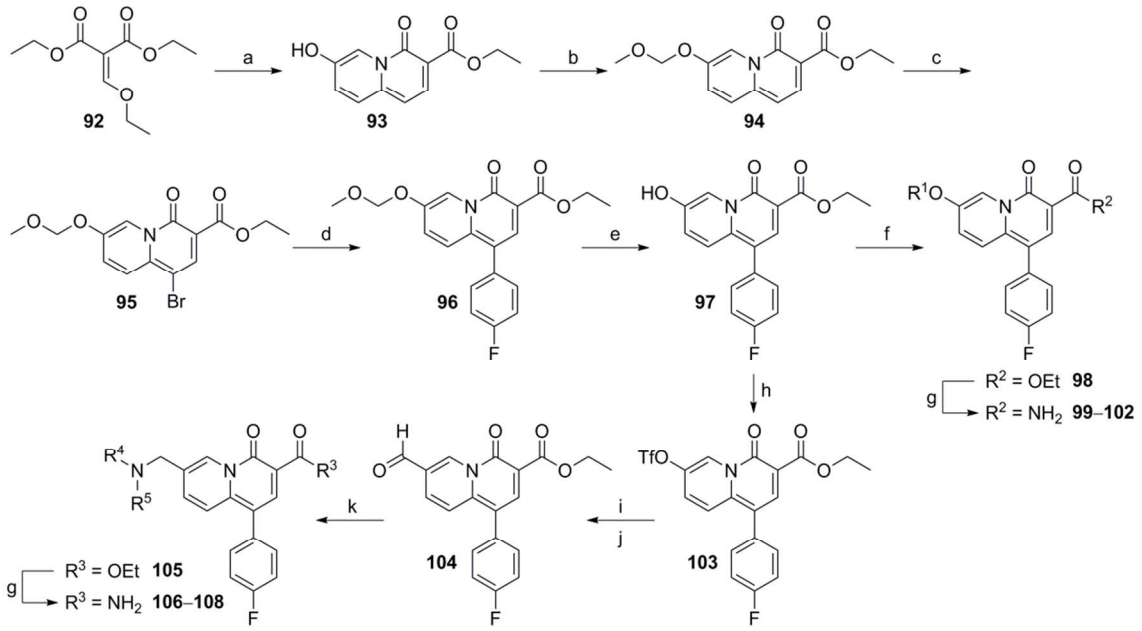

[a] Reagents and conditions: (a) 5-hydroxy-2-methylpyridine, *n*-BuLi, THF, –78 ºC to –30 ºC, 57%; (b) CH_3OCH_2Cl, DIEA, CH_2Cl_2, 0 ºC to r.t., 96%; (c) NBS, $CHCl_3$, 0 ºC to r.t., 96%; (d) 4-fluorophenylboronic acid, Pd(dppf)·CH_2Cl_2, 1M aq. Na_2CO_3, DME, 90 ºC, 94%; (e) pTSA·H_2O, EtOH, DCE, 80 ºC, 66%; (f) R^1OH, PPh_3, D^tBAD, THF, 0 ºC to 45 ºC, 38–82%; (g) 7N NH_3 in MeOH, microwave, 150 ºC, 2.0–3.0 h, 26–90%; (h) $PhN(SO_2CF_3)_2$, NEt_3, CH_2Cl_2, 0 ºC, 96%; (i) H_2CCHBF_3K, Pd(dppf)·CH_2Cl_2, NEt_3, *n*-propanol, 90 ºC, 96%; (j) OsO_4, NMO, THF, H_2O, then $NaIO_4$, 70%; (k) HNR^4R^5, $NaBH(OAc)_3$, AcOH, CH_2Cl_2, 27–67%.

$mGlu_2$ NAM Activity and Preliminary DMPK SAR. As new analogs were evaluated for potency in our functional $mGlu_2$ assay, interesting compounds were further assessed in our frontline *in vitro* drug metabolism and pharmacokinetics (DMPK) assays. Specifically, metabolic stability was determined by measuring the intrinsic clearance of the compound when incubated with rat liver microsomes (RLM).[49] The intrinsic clearance obtained was used to calculate a

predicted hepatic clearance, and compounds were binned accordingly into low (< ⅓ hepatic blood flow), moderate (⅓ to ⅔ hepatic blood flow) and high (> ⅔ hepatic blood flow) groups. The extent to which the compounds were bound to rat plasma was also measured.[50] We also calculated the lipophilicity of new analogs and attempted to assess the efficiency of the structural modifications being tested.[51] Much of the SAR work was conducted in the context of a 4-fluorophenyl ring at the 1-position of the scaffold as this was a group with good potency in the quinoline series, and it was likely to be somewhat metabolically stable. As expected, the $mGlu_2$ NAM SAR with the new 4-oxo-1,4-dihydroquinoline ether analogs showed a good deal of tolerance at the 6-position (Table 1). The ethers with directly linked heteroaryl rings (**17**–**19**) were among the least active in this set; however, *in vitro* DMPK was benchmarked. The fraction unbound in rat plasma with **17** was 0.083, and the predicted hepatic clearance was moderate. The remaining analogs **23**–**29** possessed a single sp^3 hybridized carbon between the 6-position ether oxygen and the heteroaryl ring (**A**). This feature generally improved $mGlu_2$ NAM activity. The methyl groups of analogs **24** and **25** both provided small boosts of potency relative to unsubstituted 3-pyridyl ring **23**. Analogous 4-pyridyl methyl analogs **27** and **28** were approximately two-fold more potent than unsubstituted comparator **26**. Pyrimidine analog **29** was less potent than 3-pyridyl analog **24**; however installation of this nitrogen atom reduced lipophilicity, and the ligand-lipophilicity efficiency (LLE) of **29** indicated that this 2-methylpyrimidin-5-yl functional group was worthy of continued evaluation in other analogs. The compounds examined (**24**, **25**, **27**, **28**) in our *in vitro* DMPK assays again had fraction unbound in rat plasma similar to **17**, but only **24** had moderate predicted hepatic clearance with the remaining analogs having CL_{hep} values near liver blood flow.

Table 1. $mGlu_2$ NAM and *in vitro* DMPK results with 6-substituted ethers

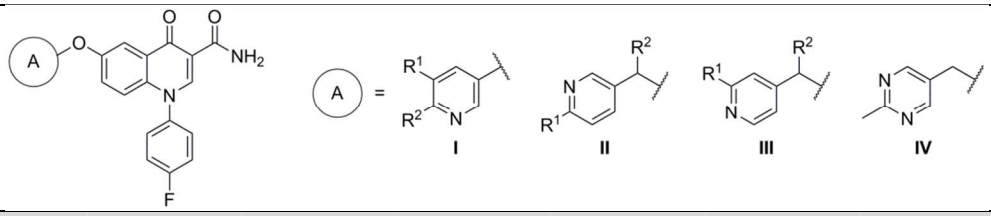

No.	A	R^1	R^2	$mGlu_2$ pIC_{50} (± SEM)[a]	$mGlu_2$ IC_{50} (nM)[a]	% Glu Max (± SEM)[a,b]	cLogP[c]	LLE[d]	rat plasma f_u[e]	rat CL_{hep} (mL/min/kg)[f]
17	I	H	H	6.07 ± 0.09	850	1.84 ± 0.47	2.80	3.27	0.083	40.6
18	I	F	H	5.89 ± 0.07	1280	0.87 ± 0.15	2.90	2.99	—	—
19	I	H	F	6.05 ± 0.12	887	1.20 ± 0.29	3.31	2.74	—	—
23	II	H	H	6.05 ± 0.07	895	1.63 ± 0.33	2.92	3.13	—	—
24	II	Me	H	6.29 ± 0.10	515	1.55 ± 0.39	3.11	3.18	0.056	43.0
25	II	H	Me	6.41 ± 0.05	386	1.31 ± 0.45	3.42	2.99	0.072	64.2
26	III	H	H	6.05 ± 0.07	895	1.63 ± 0.33	2.92	3.13	—	—
27	III	Me	H	6.39 ± 0.09	403	1.09 ± 0.16	3.11	3.28	0.091	58.0
28	III	H	Me	6.35 ± 0.06	450	1.07 ± 0.13	3.42	2.93	0.061	63.6
29	IV	—	—	6.14 ± 0.06	723	1.30 ± 0.58	2.73	3.41	—	—

[a] Calcium mobilization $mGlu_2$ assay; values are average of $n \geq 3$
[b] Amplitude of response in the presence of 30 μM test compound as a percentage of maximal response (100 μM glutamate); average of $n \geq 3$
[c] Calculated using Dotmatics Elemental (www.dotmatics.com/products/elemental/)
[d] LLE (ligand-lipophilicity efficiency) = pIC_{50} – cLogP
[e] f_u = fraction unbound
[f] Predicted hepatic clearance based on intrinsic clearance (CL_{int}) in rat liver microsomes

4-Oxo-1,4-dihydroquinoline amine analogs further illustrated the tolerance for variation at the 6-position (Table 2). Additionally, many of these analogs exhibited superior $mGlu_2$ NAM potency compared to the ether analogs discussed above. Simple alkylation of the nitrogen linker generally had minimal impact on $mGlu_2$ NAM activity as evidenced by comparing secondary amine analogs **31** and **34** to their tertiary amine comparators **32**, **35**, and **36**; however, in each case, the tertiary amine analogs exhibited a higher predicted hepatic clearance, possibly due to *N*-dealkylation. In the case of analogs with the ring (**A**) directly attached to the nitrogen linker, the 3-pyridyl ring (**32**) exhibited superior $mGlu_2$ NAM activity compared to the 4-pyridyl ring (**33**). On the other hand, the difference in potency was minimal when a methylene (**35** and **37**) or ethylene spacer (**40** and **41**) was inserted between the nitrogen atom and the ring (**A**). Combining

the methylene spacer with the 2-methylpyrimidin-5-yl ring (**38**) provided the most potent compound in this set. The fraction unbound was considerably higher with **38** relative to other similar analogs (**35** and **37**), and the predicted hepatic clearance, though still high, was less than the majority of the other analogs in this set. Though analogs **39** and **42** were not among the most potent amine analogs, these derivatives demonstrated that saturated heteroaryl rings were also tolerated at the 6-position of the chemotype.

Table 2. $mGlu_2$ NAM and *in vitro* DMPK results with 6-substituted amines

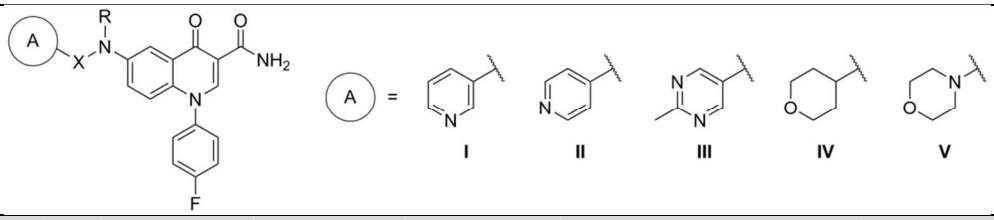

No.	A	X	R	$mGlu_2$ pIC_{50} (± SEM)[a]	$mGlu_2$ IC_{50} (nM)[a]	% Glu Max (± SEM)[a,b]	cLogP[c]	LLE[d]	rat plasma f_u[e]	rat CL_{hep} (mL/min/kg)[f]
31	I	—	H	6.48 ± 0.12	328	2.11 ± 0.42	2.57	3.91	0.084	48.2
32	I	—	Me	6.50 ± 0.37	318	–0.65 ± 1.98	2.95	3.55	0.061	60.4
33	II	—	Me	6.06 ± 0.06	874	1.16 ± 0.55	2.95	3.11	—	—
34	I	CH_2	H	6.47 ± 0.10	341	1.38 ± 0.58	2.61	3.86	0.137	51.3
35	I	CH_2	Me	6.70 ± 0.03	201	2.39 ± 0.13	2.92	3.78	0.082	67.6
36	I	CH_2	Et	6.80 ± 0.01	159	2.36 ± 0.14	3.33	3.47	0.067	68.2
37	II	CH_2	Me	6.70 ± 0.09	201	1.76 ± 0.74	2.92	3.78	0.089	67.0
38	III	CH_2	Me	6.83 ± 0.09	147	1.86 ± 0.26	2.74	4.09	0.340	47.1
39	IV	CH_2	H	6.27 ± 0.05	535	1.15 ± 0.47	2.87	3.40	—	—
40	I	CH_2CH_2	H	6.53 ± 0.12	296	1.98 ± 0.67	2.71	3.82	0.037	63.8
41	II	CH_2CH_2	H	6.42 ± 0.11	376	2.01 ± 0.40	2.71	3.71	0.172	60.5
42	V	CH_2CH_2	H	6.09 ± 0.07	816	1.13 ± 0.18	1.56	4.53	—	—

[a] Calcium mobilization $mGlu_2$ assay; values are average of $n \geq 3$
[b] Amplitude of response in the presence of 30 μM test compound as a percentage of maximal response (100 μM glutamate); average of $n \geq 3$
[c] Calculated using Dotmatics Elemental (www.dotmatics.com/products/elemental/)
[d] LLE (ligand-lipophilicity efficiency) = pIC_{50} – cLogP
[e] f_u = fraction unbound
[f] Predicted hepatic clearance based on intrinsic clearance (CL_{int}) in rat liver microsomes

Having observed that aromatic rings were not required at the 6-position, we were interested to evaluate the numerous methylene amine analogs prepared at that position. Several of these

analogs were simple tertiary amines without additional heteroatoms in the ring system (Table 3). The $mGlu_2$ NAM activity observed with these compounds was generally more dependent on minor structural changes than had been observed with previous compounds. For example, difluorocyclobutylamine **45** was approximately 5-fold more potent than cyclopentylamine **46**, and difluropyrrolidine **48** was approximately 8-fold more potent than difluoroazaspiroheptane **47**. Likewise, though unsubstituted piperidine **49** was only a weak $mGlu_2$ NAM, inhibiting the glutamate response only at the highest concentration (30 μM), further substitution of the ring with a variety of moieties enhanced potency (**50**–**54**). Three analogs (**45**, **48**, and **54**) were evaluated in our *in vitro* DMPK assays, and while the protein binding results were encouraging with more than ten percent unbound in each case, predicted hepatic clearance remained high (>48 mL/min/kg).

Table 3. $mGlu_2$ NAM and *in vitro* DMPK results with 6-substituted methylene amines

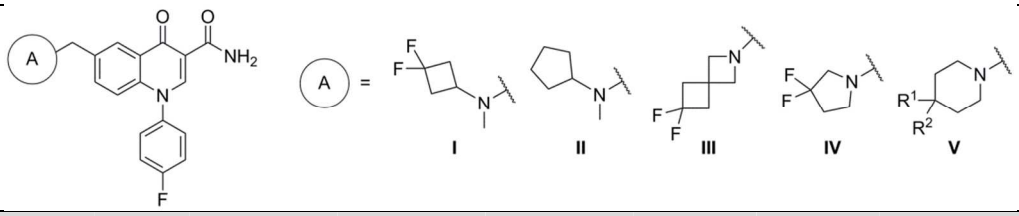

No.	A	R^1	R^2	$mGlu_2$ pIC_{50} (± SEM)[a]	$mGlu_2$ IC_{50} (nM)[a]	% Glu Max (± SEM)[a,b]	cLogP[c]	LLE[d]	rat plasma f_u[e]	rat CL_{hep} (mL/min/kg)[f]
45	I	—	—	6.40 ± 0.01	396	1.16 ± 0.18	3.86	2.54	0.138	60.9
46	II	—	—	5.66 ± 0.09	2170	0.43 ± 0.75	4.09	1.57	—	—
47	III	—	—	5.75 ± 0.06	1770	1.44 ± 0.30	3.39	2.36	—	—
48	IV	—	—	6.67 ± 0.09	214	1.10 ± 0.12	3.32	3.35	0.156	56.5
49	V	H	H	< 5.0[g]	> 10,000	37.2 ± 9.7	3.55	< 1.45	—	—
50	V	H	CF_3	6.21 ± 0.09	618	1.11 ± 0.28	4.21	2.00	—	—
51	V	H	CN	6.23 ± 0.07	587	0.90 ± 0.33	2.94	3.29	—	—
52	V	H	OMe	5.77 ± 0.11	1720	1.03 ± 0.26	3.08	2.69	—	—
53	V	H	SO_2Me	6.05 ± 0.09	886	1.36 ± 0.26	2.34	3.71	—	—
54	V	F	F	6.79 ± 0.19	161	1.59 ± 0.27	3.77	3.02	0.109	48.6

[a] Calcium mobilization $mGlu_2$ assay; values are average of n ≥ 3
[b] Amplitude of response in the presence of 30 μM test compound as a percentage of maximal response (100 μM glutamate); average of n ≥ 3
[c] Calculated using Dotmatics Elemental (www.dotmatics.com/products/elemental/)
[d] LLE (ligand-lipophilicity efficiency) = pIC_{50} – cLogP

[e] f_u = fraction unbound
[f] Predicted hepatic clearance based on intrinsic clearance (CL_{int}) in rat liver microsomes
[g] Weak activity; concentration-response curve (CRC) does not plateau

In addition to the simple tertiary amines highlighted above, we also prepared a number of analogs with heterocyclic amines (Table 4). Substituted morpholine analogs **55**–**58** were potent $mGlu_2$ NAMs with the dimethyl substituted analogs **57** and **58** offering potency superior to monomethyl analogs **55** and **56**. Particularly encouraging was analog **58**, which was predicted to be a low–moderate clearance compound in rats and was approximately 30% unbound in rat plasma. On the other hand, thiomorpholine **59** exhibited high clearance *in vitro*, and thiomorpholine 1,1-dioxide **60** showed reduced potency. We also prepared several analogs with seven-membered rings (**63**–**66**). Though most of these medium ring-containing analogs were moderate to weak $mGlu_2$ NAMs, 1,4-thiazepane **65** was quite potent. Unfortunately, **65** was highly cleared *in vitro*; however, oxidation of the sulfur atom was a likely metabolic soft-spot as clearance with 1,4-thiazepane 1,1-dioxide **66** was substantially reduced.

Table 4. $mGlu_2$ NAM and *in vitro* DMPK results with 6-substituted methylene amines (cont.)

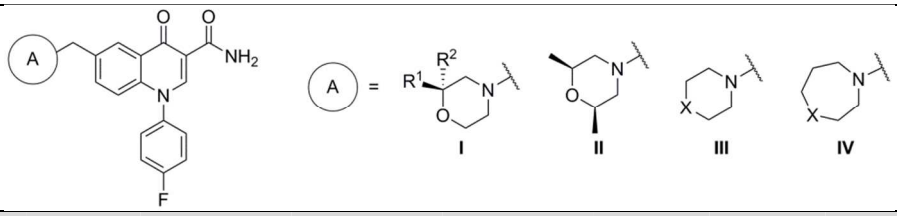

No.	A	R^1	R^2	X	$mGlu_2$ pIC_{50} (± SEM)[a]	$mGlu_2$ IC_{50} (nM)[a]	% Glu Max (± SEM)[a,b]	cLogP[c]	LLE[d]	rat plasma f_u[e]	rat CL_{hep} (mL/min/kg)[f]
55	I	Me	H	—	6.47 ± 0.16	341	0.98 ± 0.24	2.59	3.88	—	—
56	I	H	Me	—	6.26 ± 0.16	551	1.33 ± 0.15	2.59	3.67	—	—
57	I	Me	Me	—	6.93 ± 0.09	119	2.14 ± 0.17	2.99	3.94	0.16	51.2
58	II	—	—	—	6.69 ± 0.04	207	1.48 ± 0.29	3.10	3.59	0.306	24.5
59	III	—	—	S	6.38 ± 0.09	420	1.52 ± 0.63	2.76	3.62	0.205	59.6
60	III	—	—	SO_2	6.06 ± 0.08	870	1.33 ± 0.38	1.35	4.71	—	—
61	III	—	—	NMe	5.95 ± 0.06	1110	1.15 ± 0.32	2.09	3.86	—	—
62	III	—	—	NCH_2CF_3	6.21 ± 0.07	612	1.10 ± 0.07	2.90	3.31	—	—

63	IV	—	—	CH_2	5.68 ± 0.10	2080	0.55 ± 0.21	4.00	1.68	—	—
64	IV	—	—	O	< 5.0[g]	> 10,000	24.2 ± 3.6	2.54	< 2.46	—	—
65	IV	—	—	S	6.86 ± 0.10	138	2.19 ± 0.24	3.21	3.65	0.074	63.8
66	IV	—	—	SO_2	6.38 ± 0.06	415	1.24 ± 0.04	1.80	4.58	0.253	23.7

[a] Calcium mobilization $mGlu_2$ assay; values are average of n ≥ 3
[b] Amplitude of response in the presence of 30 μM test compound as a percentage of maximal response (100 μM glutamate); average of n ≥ 3
[c] Calculated using Dotmatics Elemental (www.dotmatics.com/products/elemental/)
[d] LLE (ligand-lipophilicity efficiency) = pIC_{50} – cLogP
[e] f_u = fraction unbound
[f] Predicted hepatic clearance based on intrinsic clearance (CL_{int}) in rat liver microsomes
[g] Weak activity; CRC does not plateau

Turning our attention to the 6-aryloxymethyl ether analogs **70**–**78** uncovered several additional compounds with good $mGlu_2$ NAM potency (Table 5). Several 3-pyridyl derivatives (**70**–**74**) were prepared, and 6-methyl derivative **72** and 6-chloro derivative **73** exhibited good potency. Interestingly, a trifluoromethyl group (**74**) did not function as an adequate alternative at this position. The pyridyl derivatives (**75**–**77**) demonstrated more modest differences in $mGlu_2$ NAM activity, and in this case the trifluoromethyl (**77**) was only slightly less potent than its corresponding methyl comparator (**76**). Fraction unbound with these pyridyl analogs was in line with other similar analogs (see Table 1), and predicted clearance ranged from moderate (**72** and **76**) to high (**73** and **75**). Once again, we installed a 2-methylpyrimidin-5-yl ring (**78**) and observed positive results. Specifically, not only was **78** a potent $mGlu_2$ NAM, it exhibited more than 10% fraction unbound in rat plasma and a low predicted clearance in rat liver microsomes.

Table 5. $mGlu_2$ NAM and *in vitro* DMPK results with 6-aryloxymethyl ethers

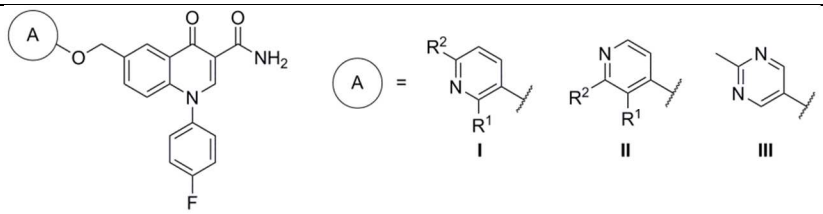

No.	A	R^1	R^2	$mGlu_2$ pIC_{50} (± SEM)[a]	$mGlu_2$ IC_{50} (nM)[a]	% Glu Max (± SEM)[a,b]	cLogP[c]	LLE[d]	rat plasma f_u[e]	rat CL_{hep} (mL/min/kg)[f]
70	I	F	H	6.13 ± 0.06	746	0.31 ± 0.30	3.42	2.71	—	—
71	I	H	F	6.35 ± 0.10	443	1.13 ± 0.38	3.42	2.93	—	—

72	I	H	Me	6.61 ± 0.11	247	1.62 ± 0.23	3.11	3.50	0.087	43.9
73	I	H	Cl	6.71 ± 0.10	193	1.70 ± 0.12	3.94	2.77	0.033	52.1
74	I	H	CF_3	5.88 ± 0.04	1330	1.23 ± 0.02	3.83	2.05	—	—
75	II	F	H	6.64 ± 0.10	228	1.83 ± 0.20	3.02	3.62	0.063	59.8
76	II	H	Me	6.45 ± 0.09	351	1.90 ± 0.32	3.11	3.34	0.050	37.2
77	II	H	CF_3	6.31 ± 0.06	486	1.70 ± 0.14	3.83	2.48	—	—
78	III	—	—	6.56 ± 0.08	277	1.71 ± 0.20	2.73	3.83	0.109	22.4

[a] Calcium mobilization $mGlu_2$ assay; values are average of n ≥ 3
[b] Amplitude of response in the presence of 30 μM test compound as a percentage of maximal response (100 μM glutamate); average of n ≥ 3
[c] Calculated using Dotmatics Elemental (www.dotmatics.com/products/elemental/)
[d] LLE (ligand-lipophilicity efficiency) = pIC_{50} – cLogP
[e] f_u = fraction unbound
[f] Predicted hepatic clearance based on intrinsic clearance (CL_{int}) in rat liver microsomes

Finally, examination of 6-ethylene linked analogs **81**–**87** yielded a range of results (Table 6). Unsubstituted phenyl analog **81** demonstrated weak $mGlu_2$ NAM activity; however, modification of the aromatic ring (**A**) to pyridine (**82** and **84**) improved potency approximately 15-fold. Unfortunately, both **82** and **84** were highly cleared *in vitro*. Substitution of 4-pyridyl analog **82** with a trifluoromethyl group (**83**) modestly enhanced potency but without reducing clearance. Substitution of 3-pyridyl analog **84** with trifluoromethyl (**85**) and fluorine (**86**) was unfavorable for $mGlu_2$ NAM activity. Again the 2-methylpyrimidin-5-yl ring (**87**) proved an attractive moiety, having demonstrated the most potent activity and highest fraction unbound in this set of analogs. Also, although predicted hepatic clearance for **87** remained on the high end, it was improved relative to other analogs in this class (**82**–**84**).

Table 6. $mGlu_2$ NAM and *in vitro* DMPK results with 6-ethylene linked analogs

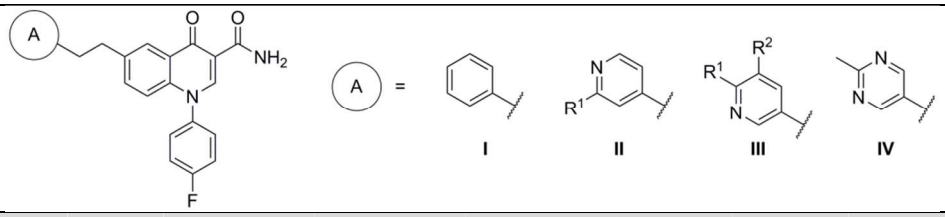

No.	A	R^1	R^2	$mGlu_2$ pIC_{50} (± SEM)[a]	$mGlu_2$ IC_{50} (nM)[a]	% Glu Max (± SEM)[a,b]	cLogP[c]	LLE[d]	rat plasma f_u[e]	rat CL_{hep} (mL/min/kg)[f]
81	I	—	—	5.16 ± 0.09	6890	2.07 ± 1.38	4.65	0.21	—	—

82	II	H	—	6.33 ± 0.09	471	1.88 ± 0.38	3.34	2.99	0.057	66.7
83	II	CF_3	—	6.52 ± 0.09	304	0.88 ± 0.06	4.25	2.27	0.039	68.4
84	III	H	H	6.33 ± 0.08	466	1.90 ± 0.11	3.34	2.99	0.062	64.1
85	III	CF_3	H	5.76 ± 0.03	1720	1.22 ± 0.14	4.25	1.51	—	—
86	III	H	F	5.93 ± 0.04	1170	0.80 ± 0.34	3.44	2.49	—	—
87	IV	—	—	6.67 ± 0.10	215	1.52 ± 0.26	3.16	3.51	0.157	46.9

[a] Calcium mobilization $mGlu_2$ assay; values are average of $n \geq 3$
[b] Amplitude of response in the presence of 30 μM test compound as a percentage of maximal response (100 μM glutamate); average of $n \geq 3$
[c] Calculated using Dotmatics Elemental (www.dotmatics.com/products/elemental/)
[d] LLE (ligand-lipophilicity efficiency) = pIC_{50} – cLogP
[e] f_u = fraction unbound
[f] Predicted hepatic clearance based on intrinsic clearance (CL_{int}) in rat liver microsomes

Having developed substantial SAR at the 6-position of the chemotype, we wanted to conduct limited exploration of another area as well. We chose ethylene linked analog **87** as a useful comparator given its overall profile. As such, additional analogs of **87** with alternative aromatic rings (**B**) to the 4-fluorophenyl ring were prepared and tested (Table 7). Replacement of the 4-fluoro group (**87**) with a 4-methoxy group (**88**) improved $mGlu_2$ NAM potency slightly, but the predicted hepatic clearance of **88** remained high. Since methoxy groups increase electron density on the ring, fluorinated analogs **89** and **90** were prepared; however, these modifications failed to improve metabolic stability. It was encouraging to see that the 4-fluorophenyl ring could be replaced altogether with a 3-methylisothiazol-5-yl ring (**91**). Analog **91** demonstrated a 2-fold drop in potency relative to **87**; yet, this modification was considered efficient by the LLE quotient as it was a less lipophilic compound. Of note, **91** had an increased fraction unbound and a marginally and perhaps insignificantly lower predicted hepatic clearance than **87**. Continued exploration of this region (**B**) of the scaffold is clearly worthwhile; however, at this point, we decided to more thoroughly profile some of the promising analogs discovered thus far to evaluate the full potential of the 4-oxo-1-aryl-1,4-dihydroquinoline-3-carboxamides as a lead series for the discovery of drug-like $mGlu_2$ NAMs.

Table 7. $mGlu_2$ NAM and *in vitro* DMPK results with modified 1-position analogs

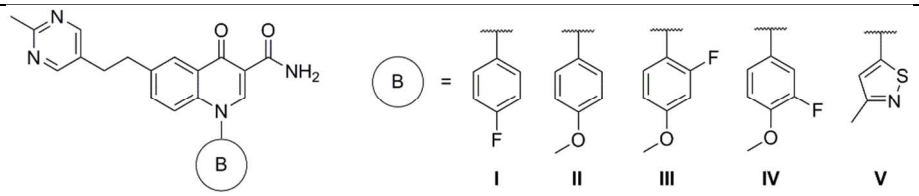

No.	B	$mGlu_2$ pIC_{50} (± SEM)[a]	$mGlu_2$ IC_{50} (nM)[a]	% Glu Max (± SEM)[a,b]	cLogP[c]	LLE[d]	rat plasma f_u[e]	rat CL_{hep} (mL/min/kg)[f]
87	**I**	6.67 ± 0.10	215	1.52 ± 0.26	3.16	3.51	0.157	46.9
88	**II**	6.87[g]	136[g]	1.61[g]	3.02	3.85	0.098	53.4
89	**III**	6.58 ± 0.09	266	1.30 ± 0.21	3.12	3.46	0.085	53.6
90	**IV**	6.70 ± 0.13	198	1.52 ± 0.38	3.12	3.58	0.159	60.5
91	**V**	6.38 ± 0.05	414	1.20 ± 0.50	2.66	3.72	0.220	41.9

[a] Calcium mobilization $mGlu_2$ assay; values are average of n ≥ 3
[b] Amplitude of response in the presence of 30 μM test compound as a percentage of maximal response (100 μM glutamate); average of n ≥ 3
[c] Calculated using Dotmatics Elemental (www.dotmatics.com/products/elemental/)
[d] LLE (ligand-lipophilicity efficiency) = pIC_{50} – cLogP
[e] f_u = fraction unbound
[f] Predicted hepatic clearance based on intrinsic clearance (CL_{int}) in rat liver microsomes
[g] Value is average of n=2

Prior to discussing the results of extended profiling of select 4-oxo-1-aryl-1,4-dihydroquinolines, it is worth briefly discussing the results obtained with the 4*H*-quinolizin-4-one analogs (Table 8). Whether in the case of the ether analogs (**99–102**) or methylene amine analogs (**106–108**), $mGlu_2$ NAM potency was consistently weak. In fact, when compared to their analogous compounds in the 4-oxo-1-aryl-1,4-dihydroquinoline series, these analogs were notably less potent in each case. These results are important because it illustrates that these two cores are not uniformly interchangeable. Moreover, it provides another example of the subtleties of SAR often seen in the design of allosteric modulators of class C GPCRs.[52–54]

Table 8. $mGlu_2$ NAM results with 4*H*-quinolizin-4-one analogs

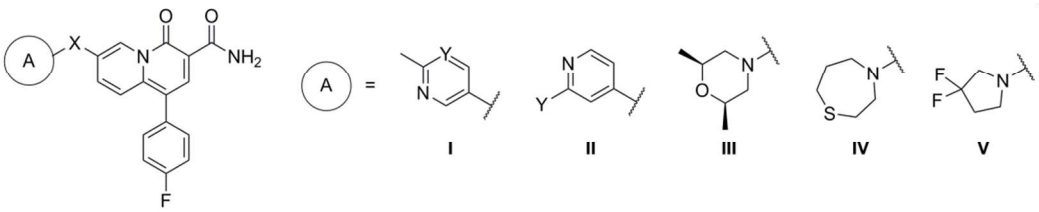

No.	A	X	Y	$mGlu_2$ pIC_{50} (± SEM)[a]	$mGlu_2$ IC_{50} (nM)[a]	% Glu Max (± SEM)[a,b]	cLogP[c]	LLE[d]	comparator[e]	fold decrease in potency[f]
99	I	O	C–H	5.40 ± 0.02	3980	2.67 ± 0.26	2.83	2.57	**24**	5.8
100	I	O	N	< 5.0[g]	> 10,000	19.4 ± 9.3	2.45	< 2.55	**29**	> 13
101	II	O	H	5.27 ± 0.07	5360	0.71 ± 1.86	2.63	2.64	**26**	6.0
102	II	O	CF_3	5.34 ± 0.01	4610	2.19 ± 0.69	3.54	1.80	—	—
106	III	CH_2	—	< 5.0[g]	> 10,000	3.95 ± 1.84	2.65	< 2.35	**58**	> 48
107	IV	CH_2	—	5.18 ± 0.13	6620	1.04 ± 2.27	2.77	2.41	**65**	48
108	V	CH_2	—	5.36 ± 0.21	4400	0.93 ± 2.27	2.87	2.49	**48**	21

[a] Calcium mobilization $mGlu_2$ assay; values are average of n ≥ 3
[b] Amplitude of response in the presence of 30 μM test compound as a percentage of maximal response (100 μM glutamate); average of n ≥ 3
[c] Calculated using Dotmatics Elemental (www.dotmatics.com/products/elemental/)
[d] LLE (ligand-lipophilicity efficiency) = pIC_{50} – cLogP
[e] Direct comparator from 4-oxo-1,4-dihydroquinoline series
[f] Fold decrease in potency relative to direct comparator from 4-oxo-1,4-dihydroquinoline series
[g] Weak activity; CRC does not plateau

Extended Characterization of Selected Analogs. In choosing the initial compounds for more in depth evaluation, we sought molecules with both promising $mGlu_2$ NAM potency and *in vitro* DMPK profiles while also desiring some structural diversity at the 6-position substituent. As such, we selected ether **17**, amine **34**, methylene amines **54** and **58**, and ethylene linked analog **87** for further profiling (Table 9). Since the potential therapeutic applications for an $mGlu_2$ NAM are in the area of CNS disorders, blood-brain barrier (BBB) penetration seemed a logical next step for evaluation in this new series. It should be noted that the fraction unbound in rat plasma ranged from 0.083 to 0.306 with these compounds; thus, consideration of unbound fraction alongside potency and CNS exposure is required to fully evaluate these compounds. Toward this end, we employed rat cassette pharmacokinetics (PK) tissue distribution studies using intravenous (IV) dosing and single time point analysis.[55] Such an approach has repeatedly proven a rapid and cost-effective mechanism for preliminary assessment of BBB penetration. In addition to the already measured protein binding in rat plasma, the protein binding of these compounds in rat brain homogenates was also assessed. Unfortunately, the observed brain to plasma ratio (K_p) for each compound was low, ranging from 0.04 (**34**) to 0.36 (**54**). Calculation of the unbound brain to unbound plasma ratio ($K_{p,uu}$) gave values that were all below 0.25,

indicating possible transporter effects.[56] Thus, analogs **58** and **87** were selected for permeability studies in Madin-Darby canine kidney (MDCK) cells transfected with the human MDR1 gene to assess potential P-glycoprotein (P-gp) mediated efflux.[57] Both compounds demonstrated substantial efflux with ratios of 52 and 44, respectively. While it was disappointing to learn that this scaffold appeared to suffer from P-gp-mediated efflux, the absolute CNS concentrations observed with **58** and its other properties raised the possibility that it might still be a valuable tool.

Table 9. Rat IV cassette and MDR1-MDCK permeability results

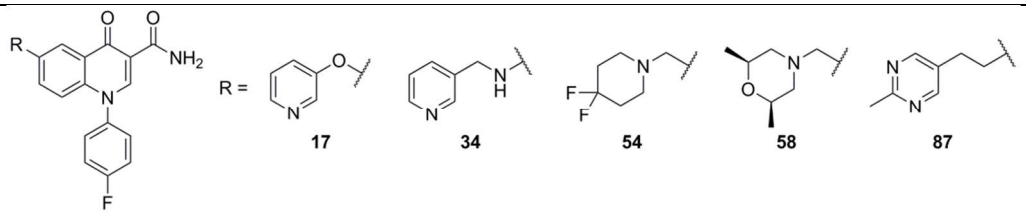

				rat IV tissue distribution results[b]				Permeability in MDR1-MDCK cells		
No.	**$mGlu_2$ IC_{50} (nM)**	**rat plasma f_u[a]**	**rat brain f_u[a]**	**plasma conc. (nM)[c]**	**brain conc. (nM)[c]**	**K_p[d]**	**$K_{p,uu}$[e]**	**A–B P_{app} (10^{-6} cm/sec)**	**B–A P_{app} (10^{-6} cm/sec)**	**Efflux Ratio**
17	850	0.083	0.087	55.8	9.2	0.16	0.17	—	—	—
34	341	0.137	0.095	83.0	3.0	0.04	0.02	—	—	—
54	161	0.109	0.068	60.5	21.6	0.36	0.22	—	—	—
58	207	0.306	0.191	56.9	18.0	0.32	0.23	1.54	79.7	52
87	215	0.157	0.160	122	5.6	0.05	0.05	1.58	69.4	44

[a] f_u = fraction unbound
[b] n = 2; dose = 0.2 mg/kg per compound; solution in 8% EtOH, 30% PEG 400, 62% DMSO (2 mg/mL total)
[c] 15 minutes post dose
[d] K_p = total brain to total plasma ratio
[e] $K_{p,uu}$ = unbound brain (brain f_u · total brain) to unbound plasma (plasma f_u · total plasma) ratio

Further profiling of compound **58** (VU6001192) began with determination of its full selectivity versus other members of the mGlu family. Selectivity versus fellow group II receptor subtype, $mGlu_3$, was particularly critical to assess. Gratifyingly, we evaluated the selectivity of **58** versus rat $mGlu_3$ using 10 point concentration-response curve (CRC) analysis in the presence of an EC_{80} concentration of glutamate, and **58** was inactive up to the highest concentration tested

(30 μM). For evaluation of selectivity versus other members of the mGlu family, the effect of 10 μM **58** on the orthosteric agonist CRC was measured in fold-shift experiments.[58,59] Fortunately, no activity at the other mGlus was noted in these assays. Because the genesis for the 4-oxo-1-aryl-1,4-dihydroquinoline chemotype as a $mGlu_2$ NAM scaffold was inspired in part by a known M_1 PAM scaffold, we also evaluated **58** in our human M_1 functional assay[60] and observed no activity up to the highest concentration tested (30 μM). Ancillary pharmacology was evaluated through screening **58** at 10 μM in a commercially available radioligand binding assay panel of 68 clinically relevant GPCRs, ion channels, kinases, and transporters,[61] and no significant responses were noted.[62]

Having established the excellent selectivity profile of **58**, we progressed the compound to additional and more definitive PK studies in both rats and mice (Table 10).[63] In spite of its predicted low–moderate clearance, a time course study using IV dosing showed **58** to be a high clearance compound; however, the volume of distribution at steady state (V_{SS}) was high and the half-life was approximately 2 hours. Thus, intraperitoneal (IP) dosing was chosen as a route that was both convenient for future use in behavioral models and had the likelihood of providing superior exposure to oral dosing. An IP tissue distribution study in rats at 30 mg/kg gave K_p and $K_{p,uu}$ values similar to those observed previously; yet, we observed a brain concentration of 760 nM, which translates to an unbound brain concentration of 145 nM and is very near the functional $mGlu_2$ IC_{50} (207 nM). An analogous study in mice at the same dose gave similar results with a brain concentration of 716 nM, which translates to an unbound brain concentration of 184 nM. Finally, to verify the role of P-gp *in vivo*, we repeated the study in mice with the modification of pre-treating the animals with the known P-gp inhibitor **109** (elacridar).[64] The

impact of this modification was profound as the exposure of **58** in the brain was increased more than 6-fold without impacting the systemic exposure in plasma.

Table 10. IV PK and tissue distribution studies with compound **58**

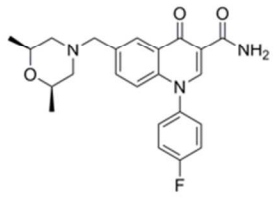

58 VU6001192

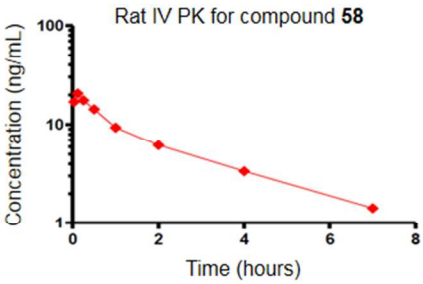

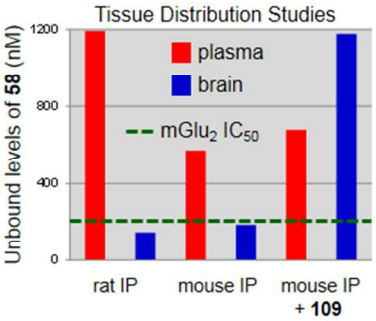

Protein Binding (f_u)[a]		Rat IV PK[b]		Rat IP Tissue Distribution[c,d]			
rat plasma	0.306	dose	0.2 mg/kg	dose		30 mg/kg	
rat brain homogenates	0.191	$t_{1/2}$	141 minutes	plasma concentration		3900 nM	
mouse plasma	0.315	CL_{plasma}	75.8 mL/min/kg	brain concentration		760 nM	
mouse brain homogenates	0.257	V_{SS}	13.3 L/kg	K_p[e]	$K_{p,uu}$[f]	0.20	0.12

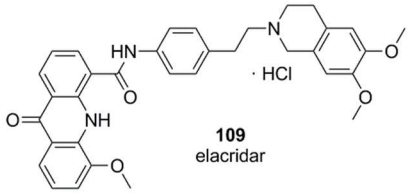

109
elacridar

Mouse IP Tissue Distribution[c,d]				Mouse IP Tissue Distribution + 109[c,d,g]			
dose		30 mg/kg		dose		30 mg/kg	
plasma concentration		1820		plasma concentration		2160	
brain concentration		716		brain concentration		4580	
K_p[e]	$K_{p,uu}$[f]	0.39	0.32	K_p[e]	$K_{p,uu}$[f]	2.1	1.7

[a] f_u = fraction unbound
[b] n = 2; solution in solution in 9% EtOH, 38% PEG 400, 53% DMSO (1 mg/mL)
[c] n = 2; fine homogenous suspension in 10% Tween80 in H_2O
[d] 15 minutes post dose of **58**
[e] K_p = total brain to total plasma ratio
[f] $K_{p,uu}$ = unbound brain (brain f_u · total brain) to unbound plasma (plasma f_u · total plasma) ratio
[g] compound **109** dosed one hour prior to compound **58** at 20 mg/kg

CONCLUSION

A potent and highly selective $mGlu_2$ NAM tool compound **58** was discovered through scaffold hopping a series in the patent literature and recognizing the possibility that an established M_1 PAM series might function as a viable chemotype for new analog design. Diverse functional groups were tolerated at the 6-position of the new chemotype, and limited work established the potential for further modifications at the 1-position. While the utility of the

compounds tested thus far is hampered by P-gp mediated efflux that limits CNS exposure, the overall profile of **58** remains interesting. The compound exhibits an unbound fraction of 25–30% in rodent brain homogenates, and a dose of 30 mg/kg using IP dosing produces unbound brain concentrations near the functional $mGlu_2$ IC_{50}. Conceivably, higher doses could be employed in order to reach pharmacologically relevant concentrations in the CNS. Perhaps more attractive is the fact that pre-treatment with a commercially available P-gp inhibitor boosts the unbound brain exposure of **58** to more than 5-fold the $mGlu_2$ IC_{50} at the same dose. The study of **58** in behavioral models relevant to $mGlu_2$ inhibition is planned and will be the subject of future communications.

EXPERIMENTAL SECTION

The synthesis of compound **58** and its associated intermediates is described below for convenience. Synthetic details for other compounds can be found in the Supporting Information.

Ethyl 3-(5-bromo-2-fluorophenyl)-3-oxopropanoate (14). 3-Ethoxy-3-oxo-propanoic acid **13** (2.16 mL, 18.3 mmol, 2.00 eq) was dissolved in THF (91 mL) in an oven dried round-bottom flask and 2,2'-bipyridyl (8.00 mg, 0.0512 mmol, 0.0056 eq) was added as an indicator. The reaction was cooled to –30 ºC and *n*-butyllithium (1.6 M in hexanes) (29.0 mL, 45.6 mmol, 4.00 eq) was added dropwise over 20 minutes. Upon final addition the reaction turned red at which point it was allowed to warm to –5 ºC. The reaction was allowed to stir at –5 ºC for 15 minutes, during which time the red color began to dissipate. Enough *n*-butyllithium was added to allow the red color to persist. The reaction was then cooled to –78 ºC and 5-bromo-2-fluoro-benzoyl chloride (2.17 g, 9.14 mmol, 1.00 eq) was added dropwise as a solution in THF (6.9 mL). The reaction was allowed to stir at –78 ºC for 30 minutes and then allowed to warm to –30 ºC and

stirred for an additional 30 minutes. The reaction was poured onto ice-cold 1N HCl (92 mL) and the mixture was extracted with ethyl acetate (1x) and DCM (2x). The combined organics were dried ($MgSO_4$), filtered and concentrated *in vacuo*. Purification by flash chromatography on silica gel afforded 1.78 g (67%) of the title compound as an off-white solid. ^{1}H NMR (400 MHz, DMSO-d_6): δ = 7.97 (dd, J = 6.5, 2.6 Hz, 1H), 7.91-7.86 (m, 1H), 7.40-7.34 (m, 1H), 4.13-4.07 (m, 4H), 1.15 ppm (t, J = 7.1 Hz, 3H). ^{13}C NMR (100 MHz, DMSO-d_6): δ = 189.68 (d, J(C,F) = 3.2 Hz), 167.09, 160.26 (d, J(C,F) = 255 Hz), 138.09 (d, J(C,F) = 9.5 Hz), 132.49 (d, J(C,F) = 2.2 Hz), 126.16 (d, J(C,F) = 13.3 Hz), 119.51 (d, J(C,F) = 25.1 Hz), 116.64, 60.71, 48.81, 13.92 ppm. HRMS (ESI): calculated for $C_{11}H_{10}BrFO_3$ [M]: 287.9797; found: 287.9794. LCMS R_T = 0.989 min, ES-MS *m/z* = 289.0 $[M+H]^+$.

Ethyl 6-bromo-1-(4-fluorophenyl)-4-oxo-1,4-dihydroquinoline-3-carboxylate (15, where Ar = 4-fluorophenyl). Compound **14** (2.87 g, 9.93 mmol, 1.00 eq) and *N,N*-dimethylformamide dimethyl acetal (1.87 mL, 14.9 mmol, 1.50 eq) were dissolved in DMF (33 mL) in a microwave vial and heated in a microwave reactor at 120 ºC for 15 minutes. To this mixture was then added 4-fluoroaniline (1.41 mL, 14.9 mmol, 1.50 eq) and the reaction was heated in a microwave reactor at 150 ºC for 20 minutes. The reaction mixture was diluted with ethyl acetate and washed with water (2x). The aqueous layers were back-extracted with ethyl acetate and the combined organics were dried ($MgSO_4$), filtered and concentrated *in vacuo*. Purification by flash chromatography on silica gel afforded 3.79 g (98%) of the title compound as yellow solid. ^{1}H NMR (400 MHz, DMSO-d_6) δ = 8.47 (s, 1H), 8.31 (d, J = 2.4 Hz, 1H), 7.81 (dd, J = 9.1, 2.4 Hz, 1H), 7.77-7.73 (m, 2H), 7.54-7.50 (m, 2H), 6.92 (d, J = 9.0 Hz, 1H), 4.20 (q, J = 7.1 Hz, 2H), 1.25 ppm (t, J = 7.1 Hz, 3H). ^{13}C NMR (100 MHz, DMSO-d_6): δ = 171.80, 163.90, 162.43 (d, J(C,F) = 247.5 Hz), 149.02, 139.70, 136.38 (d, J(C,F) = 2.8 Hz), 135.37, 130.17 (d, J(C,F) = 9.0

Hz), 128.83, 128.15, 120.73, 118.06, 117.26 (d, *J*(C,F) = 23.2 Hz), 110.88, 60.04, 14.21 ppm. HRMS (ESI): calculated for $C_{18}H_{13}BrFNO_3$ [M]: 389.0063; found: 389.0062. LCMS R_T = 0.934 min, ES-MS *m/z* = 390.2 $[M+H]^+$.

6-Bromo-1-(4-fluorophenyl)-4-oxo-1,4-dihydroquinoline-3-carboxamide (16, where Ar = 4-fluorophenyl). Ethyl 6-bromo-1-(4-fluorophenyl)-4-oxo-1,4-dihydroquinoline-3-carboxylate (1.00 g, 2.56 mmol, 1.00 eq) was suspended in 7N ammonia in methanol (30 mL) in a microwave vial and the reaction was heated in a microwave reactor at 150 ºC for 60 minutes. The reaction was concentrated to afford 881 mg (95%) of the title compound as a brown solid that was used without further purification. ^{1}H NMR (400 MHz, DMSO-d_6) δ = 9.08 (d, *J* = 4.0 Hz, 1H), 8.57 (s, 1H), 8.43 (d, *J* = 2.4 Hz, 1H), 7.85 (dd, *J* = 9.1, 2.4 Hz, 1H), 7.77-7.73 (m, 2H), 7.66 (d, *J* = 4.1 Hz, 1H), 7.56-7.50 (m, 2H), 7.02 ppm (d, *J* = 9.1 Hz, 1H). ^{13}C NMR (100 MHz, DMSO-d_6): δ = 174.64, 164.83, 162.46 (d, *J*(C,F) = 247.6 Hz), 148.42, 139.85, 136.50 (d, *J*(C,F) = 2.8 Hz), 135.66, 129.97 (d, *J*(C,F) = 9.3 Hz), 128.09, 128.07, 120.86, 118.19, 117.31 (d, *J*(C,F) = 23.3 Hz), 112.07 ppm. HRMS (ESI): calculated for $C_{16}H_{10}BrFN_2O_2$ [M]: 359.9910; found: 359.9909. LCMS R_T = 0.929 min, ES-MS *m/z* = 361.2 $[M+H]^+$.

1-(4-Fluorophenyl)-4-oxo-6-vinyl-1,4-dihydroquinoline-3-carboxamide (43, where Ar = 4-fluorophenyl). To a solution of 6-bromo-1-(4-fluorophenyl)-4-oxo-1,4-dihydroquinoline-3-carboxamide (450 mg, 1.25 mmol, 1.0 eq), triethylamine (174 µL, 1.25 mmol, 1.0 eq), and Pd(dppf)$Cl_2 \cdot CH_2Cl_2$ (18.2 mg, 0.025 mmol, 0.2 eq) in 1-propanol (8.3 mL) was added potassium vinyltrifluoroborate (200 mg, 1.5 mmol, 1.2 eq). The mixture was purged with argon and stirred at 100 ºC for 16 hours. The reaction was filtered through Celite® and washed very well with a 5%MeOH in DCM solution. The filtrate was concentrated *in vacuo* to give 385 mg (100%) of the title compound, which was used without further purification. ^{1}H NMR (400 MHz, DMSO-

d₆): δ = 9.23 (d, *J* = 4.2 Hz, 1H), 8.55 (s, 1H), 8.36 (d, *J* = 1.6 Hz, 1H), 7.89 (dd, *J* = 1.8, 8.9 Hz, 1H), 7.79-7.75 (m, 2H), 7.64 (d, *J* = 4.2 Hz, 1H), 7.54 (t, *J* = 8.7 Hz, 2H), 7.03 (d, *J* = 8.8 Hz, 1H), 6.93 (q, *J* = 11, 6.6 Hz, 1H), 5.95 (d, *J* = 17.6 Hz, 1H), 5.39 ppm (d, *J* = 11 Hz, 1H). ^{13}C NMR (100 MHz, DMSO-*d₆*): δ = 175.79, 165.17, 162.36 (d, *J*(C,F) = 247.0 Hz), 147.77, 140.24, 136.74 (d, *J*(C,F) = 3.2 Hz), 135.38, 134.17, 130.1, 129.93 (d, *J*(C,F) = 9.0 Hz), 126.74, 123.72, 118.65, 117.35 (d, *J*(C,F) = 23.4 Hz), 115.9, 111.72 ppm. HRMS (ESI): calculated for $C_{18}H_{13}FN_2O_2$ [M]: 308.0961; found: 308.0964. LCMS R_T = 0.922 min, ES-MS *m/z* = 309.2 $[M+H]^+$.

1-(4-Fluorophenyl)-6-formyl-4-oxo-1,4-dihydroquinoline-3-carboxamide (44, where Ar = 4-fluorophenyl). To a solution of 1-(4-fluorophenyl)-4-oxo-6-vinyl-1,4-dihydroquinoline-3-carboxamide (385 mg, 1.25 mmol, 1.0 eq) in 3:1 acetone/water (8 mL) was added *N*-oxide-4-methylmorpholine (220 mg, 1.87 mmol, 1.5 eq) and osmium tetroxide (6.3 mg, 0.025 mmol, 0.02 eq). After the reaction stirred for one hour, sodium periodate (294 mg, 1.37 mmol, 1.1 eq) was added. After another two hours, the reaction was diluted with EtOAc and washed well with a 10% NaS_2O_3 solution. The organic layer was dried ($MgSO_4$), filtered and concentrated *in vacuo* to give 365 mg (94%) of the title compound that was used without further purification. ^{1}H NMR (400 MHz, DMSO-*d₆*): δ = 10.17 (s, 1H), 9.10 (d, *J* = 3.8 Hz, 1H), 8.93 (d, *J* = 1.8 Hz, 1H), 8.62 (s, 1H), 8.12 (dd, *J* = 1.8, 8.8 Hz, 1H), 7.82-7.78 (m, 2H), 7.74 (d, *J* = 3.8 Hz, 1H), 7.56 (t, *J* = 8.8 Hz, 2H), 7.22 ppm (d, *J* = 8.8 Hz, 1H). ^{13}C NMR (100 MHz, DMSO-*d₆*): δ = 192.23, 175.88, 164.68, 162.49 (d, *J*(C,F) = 247 Hz), 149.06, 144.23, 136.61 (d, *J*(C,F) = 3.2 Hz), 132.48, 130.98, 130.41, 130.0 (d, *J*(C,F) = 9.3 Hz), 126.54, 119.46, 117.37 (d, *J*(C,F) = 23.3 Hz), 112.78 ppm. HRMS (ESI) calculated for $C_{17}H_{11}FN_2O_3$ [M]: 310.0754; found: 310.0757. LCMS R_T = 0.732 min, ES-MS *m/z* = 311.2 $[M+H]^+$.

6-((*cis*-2,6-Dimethylmorpholino)methyl)-1-(4-fluorophenyl)-4-oxo-1,4-dihydroquinoline-3-carboxamide (58). A solution of 1-(4-fluorophenyl)-6-formyl-4-oxo-1,4-dihydroquinoline-3-carboxamide (580 mg, 1.87 mmol, 1.0 eq) in dichloromethane (1 mL), *cis*-2,6-dimethylmorpholine (461 µL, 3.74 mmol, 2.0 eq), and acetic acid (268 µL, 4.67 mmol, 2.5 eq) was stirred for one hour. Sodium triacetoxyborohydride (594 mg, 2.80 mmol, 1.5 eq) was added. After 16 hours, the reaction was concentrated to dryness. Purification by reverse phase HPLC afforded 620 mg (81%) of the title compound as a white solid. ^{1}H NMR (400 MHz, DMSO-d_6) δ 9.23 (d, J = 4.4 Hz, 1H), 8.55 (s, 1H), 8.26 (d, J = 1.4 Hz, 1H), 7.77-7.73 (m, 2H), 7.65 (dd, J = 1.8, 8.7 Hz, 1H), 7.59 (d, J = 4.3 Hz, 1H), 7.52 (t, J = 8.7, 2H), 7.03 (d, J = 8.7, 1H), 3.57-3.52 (m, 4H), 2.65 (d, J = 10.7 Hz, 2H), 1.68 (t, J = 10.7 Hz, 2H), 1.01 ppm (d, J = 6.2 Hz, 6H). ^{13}C NMR (100 MHz, DMSO-d_6): δ = 175.8, 165.26, 162.36 (d, J(C,F) = 247 Hz), 147.78, 139.9, 136.82 (d, J(C,F) = 3.1 Hz), 135.26, 133.91, 129.98 (d, J(C,F) = 8.9 Hz), 126.41, 125.85, 118.26, 117.22 (d, J(C,F) = 23.0 Hz), 111.59, 70.97, 61.23, 58.81, 18.96 ppm. HRMS (ESI) calculated for $C_{23}H_{24}FN_3O_3$ [M]: 409.1802; found: 409.1804. LCMS R_T = 0.644 min, ES-MS *m/z* = 410.3 $[M+H]^+$.

ASSOCIATED CONTENT

Supporting Information. Experimental procedures and spectroscopic data for additional compounds, detailed molecular pharmacology, DMPK, and behavioral methods, ancillary pharmacology profile for compound **58**, ^{1}H and ^{13}C spectra for compound **58** and its associated intermediates

AUTHOR INFORMATION

Corresponding Author

* Phone: 817-735-0241. Fax: 817-735-2603. E-mail: kyle.emmitte@unthsc.edu

Present Addresses

‖ Sano Informed Prescribing, Cool Springs Life Sciences Center, 393 Nichol Mill Lane, Suite 34, Franklin, TN 37067

§ Takeda Pharmaceuticals International Co., 40 Landsdowne Street, Cambridge, MA 02139

⊥ Covance Inc., 671 South Meridian Road, Greenfield, IN 46140

Department of Pharmaceutical Sciences, UNT System College of Pharmacy, University of North Texas Health Science Center, 3500 Camp Bowie Blvd., Fort Worth, TX 76107

Author Contributions

Drs. Emmitte and Lindsley directed and designed the chemistry. Dr. Felts, Ms. Smith, and Dr. Engers performed the medicinal chemistry. Drs. Conn and Niswender directed and designed the molecular pharmacology experiments. Dr. Rodriguez directed and performed molecular pharmacology experiments. Mr. Venable performed molecular pharmacology experiments. Dr. Daniels directed and designed the DMPK experiments. Drs. Locuson and Blobaum directed DMPK experiments and performed bioanalytical work. Mr. Morrison performed bioanalytical work. Mr. Chang performed *in vitro* DMPK work. Mr. Byers performed *in vivo* DMPK work.

Funding Source

This work was generously supported by the NIMH R01MH099269 (K.A.E) and U54MH084659 (C.W.L.).

ACKNOWLEDGMENTS

We gratefully acknowledge the generous support of the National Institute of Mental Health for the funding of this work, NIMH R01MH099269 (K.A.E) and U54MH084659 (C.W.L.).

ABBREVIATIONS

7TM, seven transmembrane; Ac, acetate; BBB, blood-brain barrier Bu, butyl; CL, clearance; CNS, central nervous system; CRC, concentration response curve; dba, dibenzylideneacetone; DCE, 1,2-dichloroethane; DIEA, *N,N*-diisopropylethylamine; DME, 1,2-dimethoxyethane; DMF, *N,N*-dimethylformamide; DMPK, drug metabolism and pharmacokinetics; DMSO, dimethylsulfoxide; dppf, 1,1′-bis(diphenylphosphino)ferrocene; D^tBAD, di-*tert*-butyl azodicarboxylate; Et, ethyl; F_u, fraction unbound; GPCR, G-protein-coupled receptors; IP, intraperitoneal; IV, intravenous; K_p, brain to plasma ratio; $K_{p,uu}$, unbound brain to unbound plasma ratio; LLE, ligand-lipophilicity efficiency; M_1, muscarinic acetylcholine receptor subtype 1; max, maximum; MDCK, Madin-Darby canine kidney; MDD, major depressive disorder; Me, methyl; mGlu, metabotropic glutamate receptor; NAM, negative allosteric modulator; NBS, *N*-bromosuccinimide; NMO, *N*-methylmorpholine *N*-oxide; OCD, obsessive-compulsive disorder, PAM, positive allosteric modulator; PEG, polyethylene glycol; Ph, phenyl; P-gp, P-glycoprotein; PK, pharmacokinetics; pTSA, *p*-toluenesulfonic acid; RLM, rat liver microsomes; SAR, structure activity relationships; *t*-BuXphos, 2-di-tert-butylphosphino-2′,4′,6′-triisopropylbiphenyl; TBAF, tetrabutylammonium fluoride; THF, tetrahydrofuran; TRD, treatment-resistant depression; T, time; $t_{1/2}$, half-life; V_{SS}, volume of distribution at steady-state; Xantphos, 4,5-bis(diphenylphosphino)-9,9-dimethylxanthene.

REFERENCES

1. Niswender, C. M.; Conn, P. J. Metabotropic glutamate receptors: Physiology, pharmacology, and disease. *Annu. Rev. Pharmacol. Toxicol.* **2010**, *50*, 295–322.
2. Schoepp, D. D.; Jane, D. E.; Monn, J. A. Pharmacological agents acting at subtypes of metabotropic glutamate receptors. *Neuropharmacology* **1999**, *38*, 1431–1476.
3. Conn, P. J.; Pin, J.-P. Pharmacology and functions of metabotropic glutamate receptors. *Annu. Rev. Pharmacol. Toxicol.* **1997**, *37*, 205–237.
4. Chaki, S.; Ago, Y.; Palucha-Paniewiera, A.; Matrisciano, F.; Pilc, A. mGlu2/3 and mGlu5 receptors: Potential targets for novel antidepressants. *Neuropharmacology* **2013**, *66*, 40–52.
5. Palucha, A.; Pilc, A. Metabotropic glutamate receptor ligands as possible anxiolytic and antidepressant drugs. *Pharmacol. Ther.* **2007**, *115*, 116–147.
6. Ellaithy, A.; Younkin, J.; Gónazlez-Maeso, J.; Logothetis, D. E. Positive allosteric modulators of metabotropic glutamate 2 receptors in schizophrenia treatment. *Trends Neurosci.* **2015**, *38*, 506−516.
7. Célanire, S.; Sebhat, I.; Wichmann, J.; Mayer, S.; Schann, S.; Gatti, S. Novel metabotropic glutamate receptor 2/3 antagonists and their therapeutic applications: a patent review (2005 – present). *Expert Opin. Ther. Pat.* **2015**, *25*, 69–90.
8 . Ornstein, P. L.; Bleisch, T. J.; Arnold, M. B.; Kennedy, J. H.; Wright, R. A.; Johnson, B. G.; Tizzano, J. P.; Helton, D. R.; Kallman, M. J.; Schoepp, D. D. 2-Substituted (2*SR*)-2-amino-2-((1*SR*,2*SR*)-2-carboxycycloprop-1-yl)glycines as potent and selective antagonists of group II metabotropic glutamate receptors. 2. Effects of aromatic substitution, pharmacological characterization, and bioavailability. *J. Med. Chem.* **1998**, *41*, 358–378.

9. Chaki, S.; Yoshikawa, R.; Hirota, S.; Shimazaki, T.; Maeda, M.; Kawashima, N.; Yoshimizu, T.; Yasuhara, A.; Sakagami, K.; Okuyama, S.; Nakanishi, S.; Nakazato, A. MGS0039: a potent and selective group II metabotropic glutamate receptor antagonist with antidepressant-like activity. *Neuropharmacology* **2004**, *46*, 457–467.

10. Bespalov, A. Y.; van Gaalen, M. M.; Sukhotina, I. A.; Wicke, K.; Mezler, M.; Schoemaker, H; Gross, G. Behavioral characterization of the mGlu group II/III receptor antagonist, LY-341495, in animal models of anxiety and depression. *Eur. J. Pharmacol.* **2008**, *592*, 96–102.

11. Shimazaki, T.; Iijima, M.; Chaki, S. Anxiolytic-like activity of MGS0039, a potent group II metabotropic glutamate receptor antagonist, in a marble-burying behavior test. *Eur. J. Pharmacol.* **2004**, *501*, 121–125.

12. Yoshimizu, T.; Shimazaki, T.; Ito, A.; Chaki, S. An mGluR2/3 antagonist, MGS0039, exerts antidepressant and anxiolytic effects in behavioral models in rats. *Psychopharmacology* **2006**, *186*, 587–593.

13. Higgins, G. A.; Ballard, T. M.; Kew, J. N.; Richards, J. G.; Kemp, J. A.; Adam, G.; Woltering, T.; Nakanishi, S.; Mutel, V. Pharmacological manipulation of mGlu2 receptors influences cognitive performance in the rodent. *Neuropharmacology* **2004**, *46*, 907–917.

14. Kim, S. H.; Steele, J. W.; Lee, S. W.; Clemenson, G. D.; Carter, T. A.; Treuner, K.; Gadient, R.; Wedel, P.; Glabe, C.; Barlow, C.; Ehrlich, M. E.; Gage, F. H.; Gandy, S. Proneurogenic group II mGluR antagonist improves learning and reduces anxiety in Alzheimer Aβ oligomer mouse. *Mol. Psychiatry* **2014**, *19*, 1235–1242.

15. Kim, S. H.; Fraser, P. E.; Westaway, D.; St. George-Hyslop, P. H.; Ehrlich, M. E.; Gandy, S. Group II metabotropic glutamate receptor stimulation triggers production and release of

Alzheimer's amyloid β_{42} from isolated intact nerve terminals. *J. Neurosci.* **2010**, *30*, 3870–3875.

16. Yoshimizu, T.; Chaki, S. Increased cell proliferation in the adult mouse hippocampus following chronic administration of group II metabotropic glutamate receptor antagonist, MGS0039. *Biochem. Biophys. Res. Comm.* **2004**, *315*, 493–496.
17. Gleason, S. D.; Li, X.; Smith, I. A.; Ephlin, J. D.; Wang, X. S.; Heinz, B. A.; Carter, J. H.; Baez, M.; Yu, J.; Bender, D. M.; Witkin, J. M. mGlu2/3 agonist-induced hyperthermia: An in vivo assay for detection of mGlu2/3 receptor antagonism and its relation to antidepressant-like efficacy in mice. *CNS Neurol. Disord. Drug Targets* **2013**, *12*, 554–566.
18. Koike, H.; Fukumoto, K.; Iijima, M.; Chaki, S. Role of BDNF/TrkB signaling in antidepressant-like effects of a group II metabotropic glutamate receptor antagonist in animal models of depression. *Behav. Brain Res.* **2013**, *238*, 48–52.
19. Koike, H.; Iijima, M.; Chaki, S. Involvement of the mammalian target of rapamycin signaling in the antidepressant-like effect of group II metabotropic glutamate receptor antagonists. *Neuropharmacology* **2011**, *61*, 1419–1423.
20. Karasawa, J.; Shimazaki, T.; Kawashima, N.; Chaki, S. AMPA receptor stimulation mediates the antidepressant-like effect of a group II metabotropic glutamate receptor antagonist. *Brain Res.* **2005**, *1042*, 92–98.
21. Iijima, M.; Koike, H.; Chaki, S. Effect of an mGlu2/3 receptor antagonist on depressive behavior induced by withdrawal from chronic treatment with methamphetamine. *Behav. Brain Res.* **2013**, *246*, 24–28.
22. Markou, A. Metabotropic glutamate receptor antagonists: Novel therapeutics for nicotine dependence and depression? *Biol. Psychiatry* **2007**, *61*, 17–22.

23. Ago Y.; Yano, K.; Araki, R.; Hiramatsu, N.; Kita, Y.; Kawasaki, T.; Onoe, H.; Chaki, S.; Nakazato, A.; Hashimoto, H.; Baba, A.; Takuma, K.; Matsuda, T. Metabotropic glutamate 2/3 receptor antagonists improve behavioral and prefrontal dopaminergic alterations in the chronic corticosterone-induced depression model in mice. *Neuropharmacology* **2013**, *65*, 29–38.

24. Dwyer, J. M.; Lepack, A. E.; Duman, R. S. mGluR2/3 blockade produces rapid and long-lasting reversal of anhedonia caused by chronic stress exposure. *J. Mol. Psychiatry* **2013**, *1*, No. 15.

25. Campo, B.; Kalinichev, M.; Lambeng, N.; Yacoubi, M. E.; Royer-Urios, I.; Schneider, M.; Legrand, C.; Parron, D.; Girard F.; Bessif, A.; Poli, S.; Vaugeois, J.-M.; Le Poul, E.; Célanire, S. Characterization of an mGluR2/3 negative allosteric modulator in rodent models of depression. *J. Neurogenet.* **2011**, *25*, 152–166.

26. Pritchett, D.; Jagannath, A.; Brown, L. A.; Tam, S. K. E.; Hasan, S.; Gatti, S.; Harrison, P. J.; Bannerman, D. M.; Foster, R. G.; Peirson, S. N. Deletion of metabotropic glutamate receptors 2 and 3 (mGlu2 & mGlu3) in mice disrupts sleep and wheel-running activity, and increases the sensitivity of the circadian system to light. *PLoS One* **2015**, *10*, e0125523(1-21).

27. Woltering, T. J.; Wichmann, J.; Goetschi, E.; Knoflach, F.; Ballard, T. M.; Huwyler, J.; Gatti S. Synthesis and characterization of 1,3-dihydro-benzo[*b*][1,4]diazepin-2-one derivatives: Part 4. In vivo active potent and selective non-competitive metabotropic glutamate receptor 2/3 antagonists. *Bioorg. Med. Chem. Lett.* **2010**, *20*, 6969–6974.

28. Yacoubi, M. E.; Vaugeois, J.-M.; Kalinichev, M.; Célanire, S.; Parron, D.; Le Poul, E.; Campo, B. Effects of a mGluR2/3 negative allosteric modulator and a reference mGluR2/3

orthosteric antagonist in a genetic mouse model of depression. In *Behavioral Studies of Mood Disorders*, Proceedings of the 40th Annual Meeting of the Society for Neuroscience, San Diego, CA, Nov 13–17, 2010; Society for Neuroscience: Washington, DC, 2010; 886.14/VV7.

29. Goeldner, C.; Ballard, T. M.; Knoflach, F.; Wichmann, J.; Gatti, S.; Umbricht, D. Cognitive impairment in major depression and the mGlu2 receptor as a therapeutic target. *Neuropharmacology* **2013**, *64*, 337–346.
30. Kalinichev, M.; Campo, B.; Lambeng, N.; Célanire, S.; Schneider, M.; Bessif, A.; Royer-Urios, I.; Parron, D.; Legrand, C.; Mahious, N.; Girard, F.; Le Poul, E. An mGluR2/3 negative allosteric modulator improves recognition memory assessed by natural forgetting in the novel object recognition test in rats. In *Memory Consolidation and Reconsolidation: Molecular Mechanisms II*, Proceedings of the 40th Annual Meeting of the Society for Neuroscience, San Diego, CA, Nov 13–17, 2010; Society for Neuroscience: Washington, DC, 2010; 406.9/MMM57.
31. Structure of decoglurant disclosed in Recommended International Nonproprietary Names (INN). *WHO Drug Information*; Vol. 27, No. 3; World Health Organization: Geneva, Switzerland, 2013; 150.
32. ClinicalTrials.gov: ARTDeCo Study: A study of RO4995819 in patients with major depressive disorder and inadequate response to ongoing antidepressant treatment. https://www.clinicaltrials.gov/ct2/show/NCT01457677 (accessed August 12, 2015).
33. Sheffler, D. J.; Wenthur, C. J.; Bruner, J. A.; Carrington, S. J. S.; Vinson, P. N.; Gogi, K. K.; Blobaum, A. L.; Morrison, R. D.; Vamos, M.; Cosford, N. D. P.; Stauffer, S. R.; Daniels, J. S.; Niswender, C. M.; Conn, P. J.; Lindsley, C. W. Development of a novel, CNS-penetrant,

metabotropic glutamate receptor 3 ($mGlu_3$) NAM probe (ML289) derived from a closely related $mGlu_5$ PAM. *Bioorg. Med. Chem. Lett.* **2012**, *22*, 3921–3925.

34. Wenthur, C. J.; Morrison, R.; Felts, A. S.; Smith, K. A.; Engers, J. L.; Byers, F. W.; Daniels, J. S.; Emmitte, K. A.; Conn, P. J.; Lindsley, C. W. Discovery of (*R*)-(2-fluoro-4-((-4-methoxyphenyl)ethynyl)phenyl(3-hydroxypiperidin-1-yl)methanone (ML337), An $mGlu_3$ selective and CNS penetrant negative allosteric modulator (NAM). *J. Med. Chem.* **2013**, *56*, 5208–5212.
35. Walker, A. G.; Wenthur, C. J.; Xiang, Z.; Rook, J. M.; Emmitte, K. A.; Niswender, C. M.; Lindsley, C. W.; Conn, P. J. Metabotropic glutamate receptor 3 activation is required for long-term depression in medial prefrontal cortex and fear extinction. *Proc. Natl. Acad. Sci. U.S.A.* **2015**, *112*, 1196–1201.
36. Engers, J. L.; Rodriguez, A. L.; Konkol, L. C.; Morrison, R. D.; Thompson, A. D.; Byers, F. W.; Blobaum, A. L.; Chang, S.; Venable, D. F.; Loch, M. T.; Niswender, C. M.; Daniels, J. S.; Jones, C. K.; Conn, P. J.; Lindsley, C. W.; Emmitte, K. A. Discovery of a selective and CNS penetrant negative allosteric modulator of metabotropic glutamate receptor subtype 3 with antidepressant and anxiolytic activity in rodents. *J. Med. Chem.* **2015**, *58*, 7485–7500.
37. Bungard, C. J.; Converso, A.; De Leon, P.; Hanney, B.; Hartingh, T. J.; Manikowski, J. J.; Manley, P. J.; Meissner, R.; Meng, Z.; Perkins, J. J.; Rudd, M. T.; Shu, Y. Quinoline carboxamide and quinoline carbonitrile derivatives as mGluR2-negative allosteric modulators, compositions, and their use. PCT Int. Pat. Appl. WO 2013/066736 A1, May 10, 2013.

38. Kuduk, S. D.; Di Marco, C. N.; Cofre, V.; Ray, W. J.; Ma, L.; Wittmann, M.; Seager, M. A.; Koeplinger, K. A.; Thompson, C. D.; Hartman, G. D.; Bilodeau, M. T. Fused heterocyclic M_1 positive allosteric modulators. *Bioorg. Med. Chem. Lett.* **2011**, *21*, 2769–2772.

39. Kuduk, S. D.; Di Marco, C. N.; Chang, R. K.; Ray, W. J.; Ma, L.; Wittmann, M.; Seager, M. A.; Koeplinger, K. A.; Thompson, C. D.; Hartman, G. D.; Bilodeau, M. T. Heterocyclic fused pyridone carboxylic acid M_1 positive allosteric modulators. *Bioorg. Med. Chem. Lett.* **2010**, *20*, 2533–2537.

40. Yang, F. V.; Shipe, W. D.; Bunda, J. L.; Nolt, M. B.; Wisnoski, D. D.; Zhao, Z.; Barrow, J. C.; Ray, W. J.; Ma, L.; Wittman, M.; Seager, M. A.; Koeplinger, K. A.; Hartman, G. D.; Lindsley, C. W. Parallel synthesis of N-biaryl quinolone carboxylic acids as selective M_1 positive allosteric modulators. *Bioorg. Med. Chem. Lett.* **2010**, *20*, 531–536.

41. Anderson, K. W.; Ikawa, T.; Tundel, R. E.; Buchwald, S. L. The selective reaction of aryl halides with KOH: Synthesis of phenols, aromatic ethers, and benzofurans. *J. Am. Chem. Soc.* **2006**, *128*, 10694–10695.

42. But, T. Y. S.; Toy, P. H. The Mitsunobu reaction: Origin, mechanism, improvements, and applications. *Chem. Asian J.* **2007**, *2*, 1340–1355.

43. Surry, D. S.; Buchwald, S. L. Biaryl phosphane ligands in palladium-catalyzed amination. *Angew. Chem. Int. Ed.* **2008**, *47*, 6338–6361.

44. Rodríguez Rivero, M.; Molander, G. A. Suzuki cross-coupling reactions of potassium alkenyltrifluoroborates. *Org. Lett.* **2002**, *4*, 107–109.

45. Thorand, S.; Krause, N. Improved procedures for the palladium-catalyzed coupling of terminal alkynes with aryl bromides (Sonogashira coupling). *J. Org. Chem.* **1998**, *63*, 8551–8553.

46. Kuduk, S. D.; Chang, R. K.; Di Marco, C. N.; Pitts, D. R.; Greshock, T. J.; Ma, L.; Wittmann, M.; Seager, M. A.; Koeplinger, K. A.; Thompson, C. D.; Hartman, G. D.; Bilodeau, M. T.; Ray, W. J. Discovery of a selective allosteric M_1 receptor modulator with suitable development properties based on a quinolizidinone carboxylic acid scaffold. *J. Med. Chem.* **2011**, *54*, 4773–4780.

47. Kuduk, S. D.; Chang, R. K.; Di Marco, C. N.; Ray, W. J.; Ma, L.; Wittmann, M.; Seager, M. A.; Koeplinger, K. A.; Thompson, C. D.; Hartman, G. D.; Bilodeau, M. T. Quinolizidinone carboxylic acid selective M_1 allosteric modulators: SAR in the piperidine series. *Bioorg. Med. Chem. Lett.* **2011**, *21*, 1710–1715.

48. Kuduk, S. D.; Chang, R. K.; Di Marco, C. N.; Ray, W. J.; Ma, L.; Wittmann, M.; Seager, M. A.; Koeplinger, K. A.; Thompson, C. D.; Hartman, G. D.; Bilodeau, M. T. Quinolizidinone carboxylic acids as CNS penetrant, selective M_1 allosteric muscarinic receptor modulators. *ACS Med. Chem. Lett.* **2010**, *1*, 263–267.

49. Obach, R. S. Prediction of human clearance of twenty-nine drugs from hepatic microsomal intrinsic clearance data: An examination of in vitro half-life approach and nonspecific binding to microsomes. *Drug Metab. Dispos.* **1999**, *27*, 1350–1359.

50. Kalvass, J. C.; Maurer, T. S. Influence of nonspecific brain and plasma binding on CNS exposure: implications for rational drug discovery. *Biopharm. Drug Dispos.* **2002**, *23*, 327–338.

51. Leeson, P. D.; Springthorpe, B. The influence of drug-like concepts on decision-making in medicinal chemistry. *Nat. Rev. Drug Discovery* **2007**, *6*, 881–890.

52. Stauffer, S. L. Progress toward positive allosteric modulators of the metabotropic glutamate receptor subtype 5 ($mGlu_5$). *ACS Chem. Neurosci.* **2011**, *2*, 450–470.

53. Robichaud, A. J.; Engers, D. W.; Lindsley, C. W.; Hopkins, C. R. Recent progress on the identification of metabotropic glutamate 4 receptor ligands and their potential utility as CNS therapeutics. *ACS Chem. Neurosci.* **2011**, *2*, 433–449.

54. Emmitte, K. A. Recent advances in the design and development of novel negative allosteric modulators of $mGlu_5$. *ACS Chem. Neurosci.* **2011**, *2*, 411–432.

55. Bridges, T. M.; Morrison, R. D.; Byers, F. W.; Luo, S.; Daniels, J. S. Use of a novel rapid and resource-efficient cassette dosing approach to determine the pharmacokinetics and CNS distribution of small molecule 7-transmembrane receptor allosteric modulators in rat. *Pharmacol. Res. Perspect.* **2014**, *2*, e00077(1-9).

56. Di, L.; Rong, H.; Feng, B. Demystifying brain penetration in central nervous system drug discovery. *J. Med. Chem.* **2013**, *56*, 2–12.

57. Wang, Q.; Rager, J. D.; Weinstein, K.; Kardos, P. S.; Dobson, G. L.; Li, J.; Hidalgo, I. J. Evaluation of the MDR-MDCK cell line as a permeability screen for the blood–brain barrier. *Int. J. Pharm.* **2005**, *288*, 349–359.

58. Noetzel, M. J.; Rook, J. M.; Vinson, P. N.; Cho, H.; Days, E.; Zhou, Y.; Rodriguez, A. L.; Lavreysen, H.; Stauffer, S. R.; Niswender, C. M.; Xiang, Z.; Daniels, J. S.; Lindsley, C. W.; Weaver, C. D.; Conn, P. J. Functional impact of allosteric agonist activity of selective positive allosteric modulators of metabotropic glutamate receptor subtype 5 in regulating central nervous system function. *Mol. Pharmacol.* **2012**, *81*, 120–133.

59. Niswender, C.M.; Johnson, K. A.; Luo, Q.; Ayala, J. E.; Kim, C.; Conn, P. J.; Weaver, C. D. A novel assay of Gi/o-linked G protein-coupled receptor coupling to potassium channels provides new insights into the pharmacology of the group III metabotropic glutamate receptors. *Mol. Pharmacol.* **2008**, *73,* 1213–1224.

60. Tarr, J. C.; Turlington, M. L.; Reid, P. R.; Utley, T. J.; Sheffler, D. J.; Cho, H. P.; Klar, R.; Pancani, T.; Klein, M. T.; Bridges, T. M.; Morrison, R. D.; Blobaum, A. L.; Xiang, Z.; Daniels, J. S.; Niswender, C. M.; Conn, P. J.; Wood, M. R.; Lindsley, C. W. Targeting selective activation of M_1 for the treatment of Alzheimer's disease: Further chemical optimization and pharmacological characterization of the M_1 positive allosteric modulator ML169. *ACS Chem. Neurosci.* **2012**, *3*, 884–895.

61. LeadProfilingScreen® (catalog #68), Eurofins Panlabs, Inc. (www.eurofinspanlabs.com)

62. Significant responses are defined as those that inhibited more than 50% of radioligand binding.

63. Bridges, T. M.; Rook, J. M.; Noetzel, M. J.; Morrison, R. D.; Zhou, Y.; Gogliotti, R. D.; Vinson, P. N.; Xiang, Z.; Jones, C. K.; Niswender, C. M.; Lindsley, C. W.; Stauffer, S. L.; Conn, P. J.; Daniels, J. S. Biotransformation of a novel positive allosteric modulator of metabotropic glutamate receptor subtype 5 contributes to seizure-like adverse events in rats involving a receptor agonism-dependent mechanism. *Drug Metab. Dispos.* **2013**, *41*, 1703–1714.

64. Kallem, R.; Kulkarni, C. P.; Patel, D.; Thakur, M.; Sinz, M.; Singh, S. P.; Mahammad, S. S.; Mandlekar, S. A simplified protocol employing elacridar in rodents: A screening model in drug discovery to assess P-gp mediated efflux at the blood brain barrier. *Drug Metab. Lett.* **2012**, *6*, 134–144.

TABLE OF CONTENTS GRAPHIC

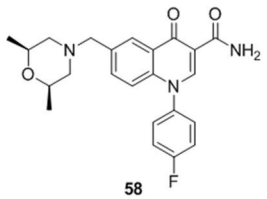

58

$mGlu_2$ IC_{50} = 207 nM

$mGlu_3$ IC_{50} > 30 μM

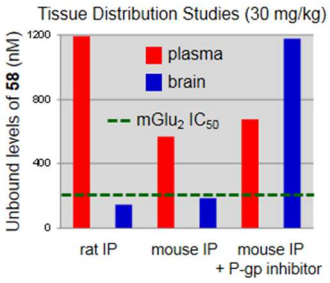

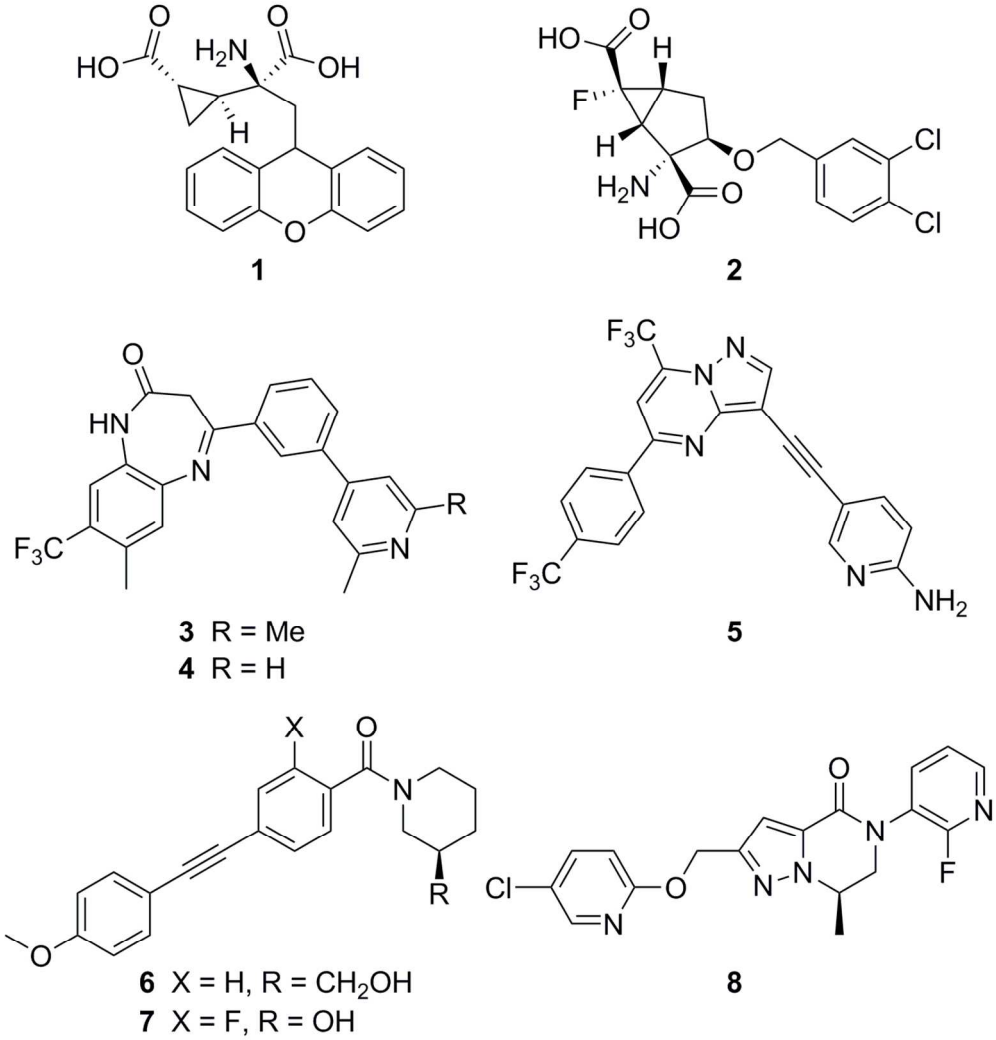

Figure 1. $mGlu_{2/3}$ orthosteric antagonist tools **1** and **2**, $mGlu_{2/3}$ NAM tools **3** and **4**, Roche $mGlu_{2/3}$ NAM clinical compound **5**, first-generation selective $mGlu_3$ NAMs **6** and **7**, and $mGlu_3$ NAM *in vivo* tool **8**.
121x127mm (300 x 300 DPI)

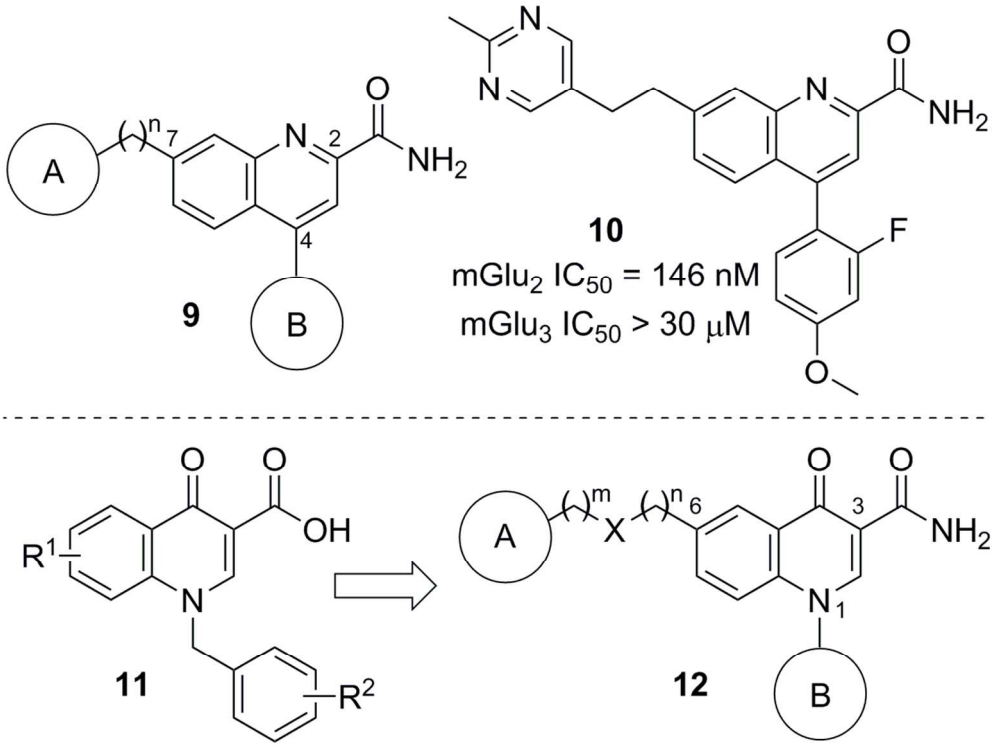

Figure 2. Merck quinoline-2-carboxamide $mGlu_2$ NAM scaffold **9** and representative compound **10**; Merck 4-oxo-1,4-dihydroquinoline-3-carboxylic acid M_1 PAM scaffold **11**; Proposed 4-oxo-1-aryl-1,4-dihydroquinoline-3-carboxamide $mGlu_2$ NAM scaffold.
107x81mm (300 x 300 DPI)

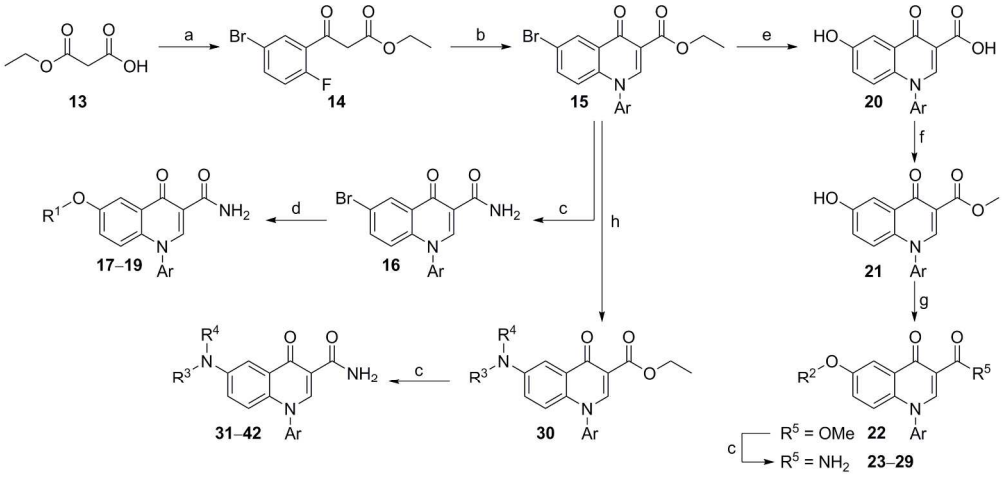

Scheme 1. Synthesis of 6-heteroatom linked analogs[a]
211x100mm (300 x 300 DPI)

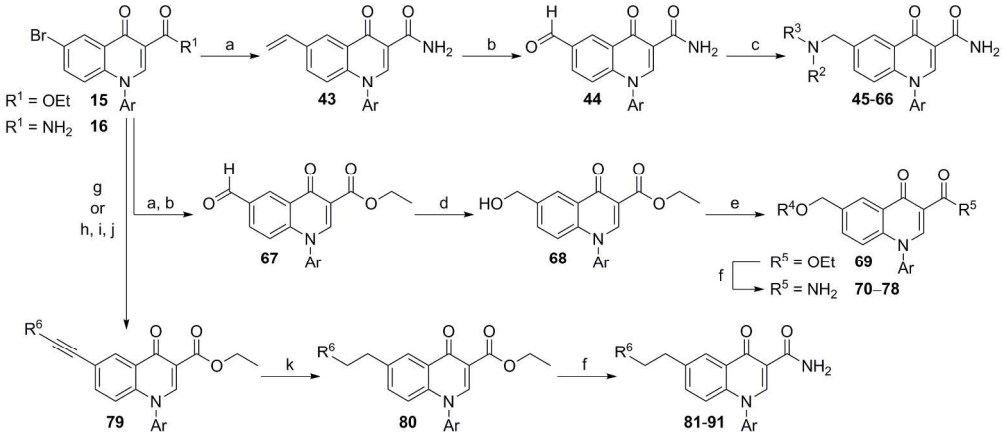

Scheme 2. Synthesis of 6-carbon linked analogs[a]
217x94mm (300 x 300 DPI)

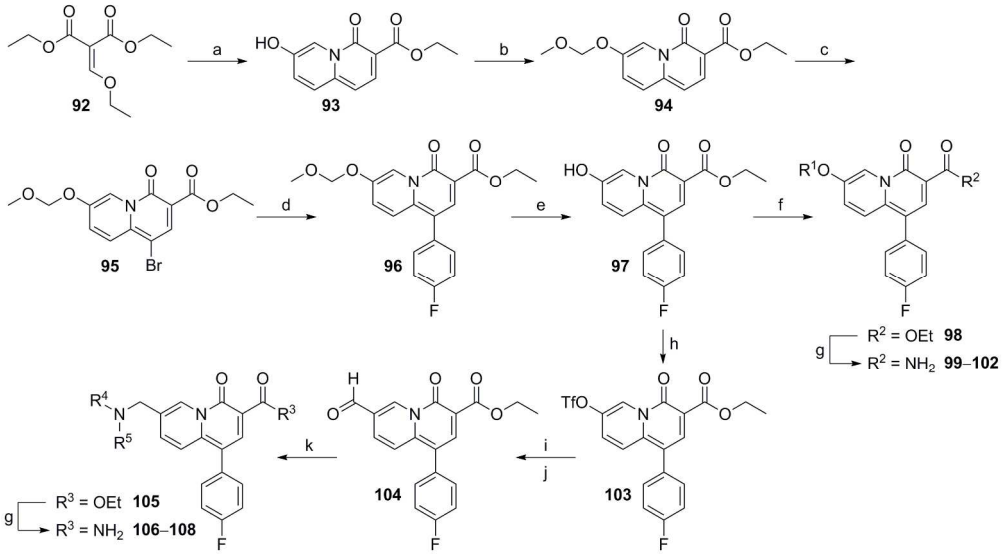

Scheme 3. Synthesis of 4*H*-quinolizin-4-one analogs[a]
215x119mm (300 x 300 DPI)

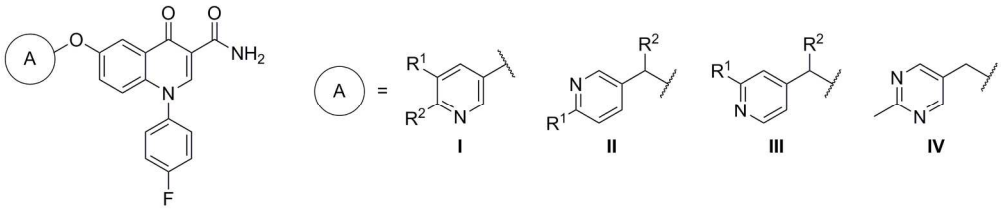

191x40mm (300 x 300 DPI)

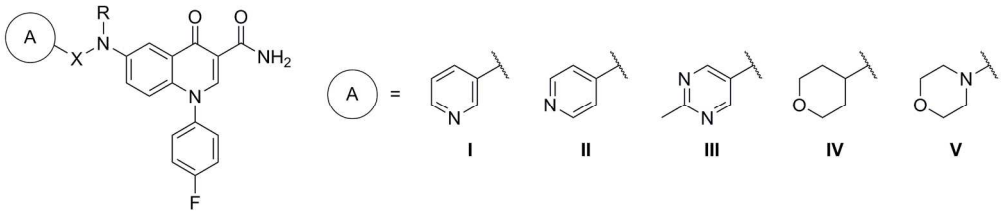

192x40mm (300 x 300 DPI)

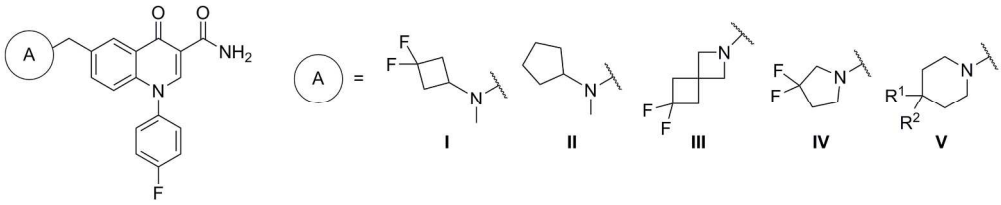

197x40mm (300 x 300 DPI)

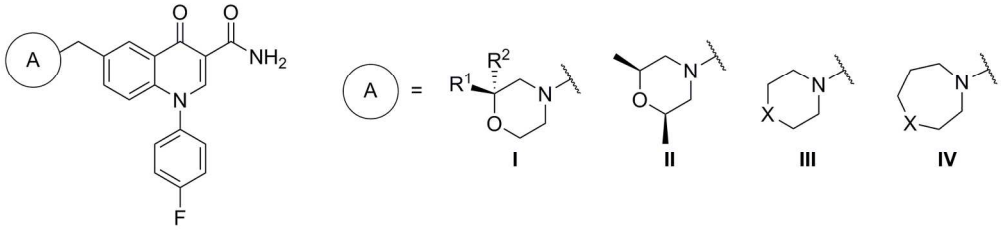

173x40mm (300 x 300 DPI)

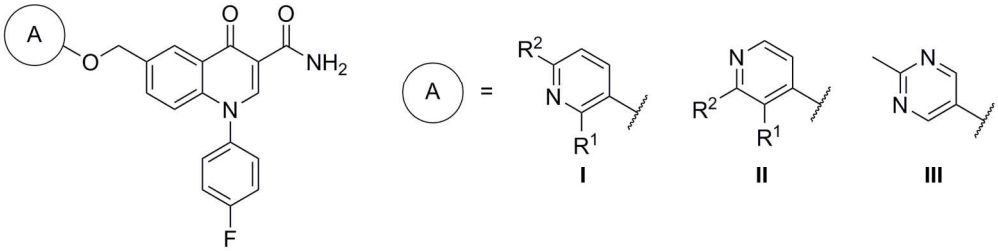

157x40mm (300 x 300 DPI)

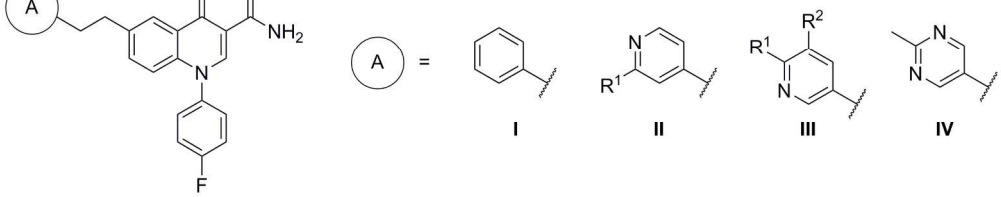

181x40mm (300 x 300 DPI)

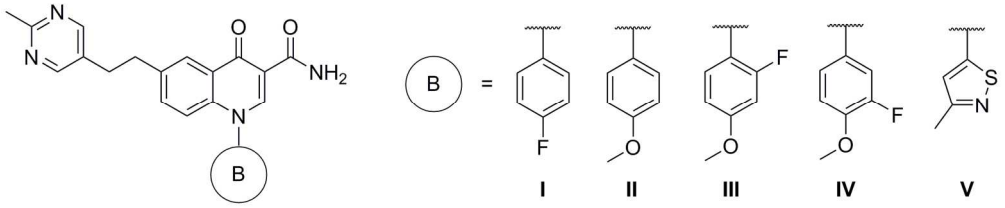

170x35mm (300 x 300 DPI)

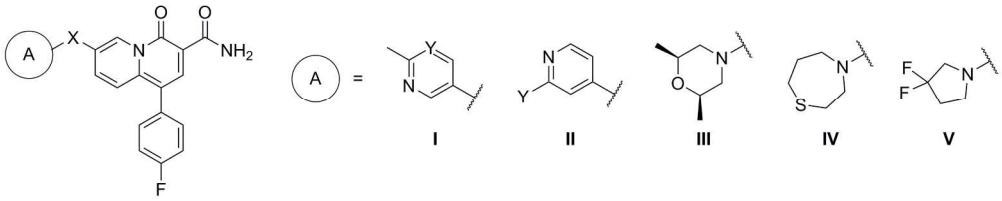

200x40mm (300 x 300 DPI)

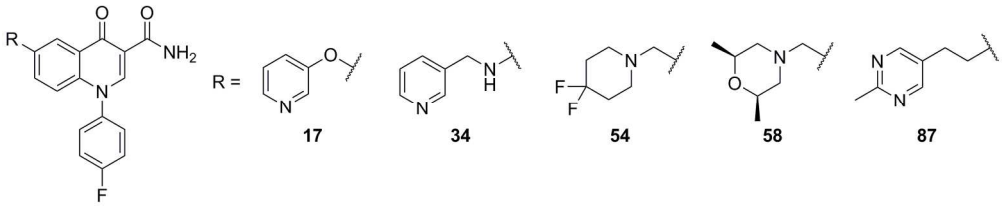

195x40mm (300 x 300 DPI)

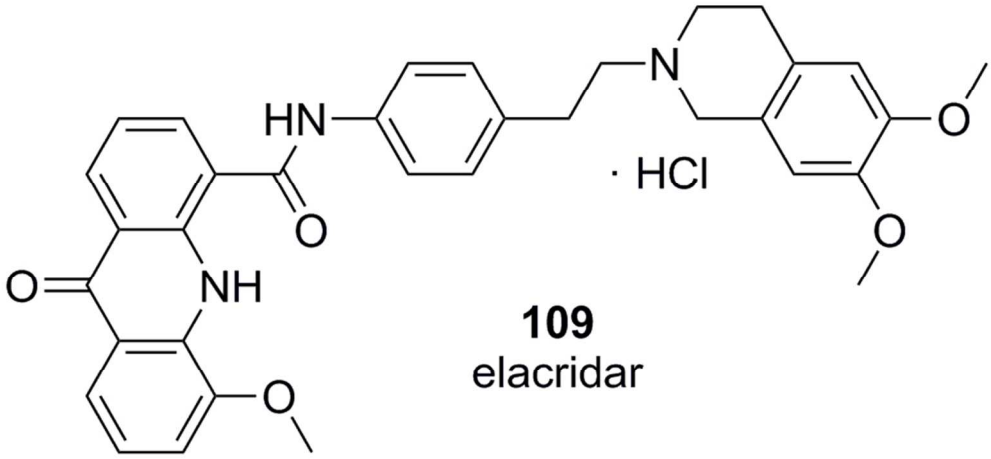

109
elacridar

79x36mm (300 x 300 DPI)

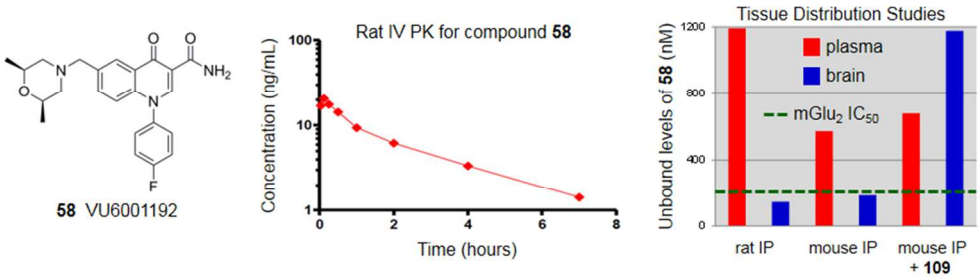

191x55mm (120 x 120 DPI)

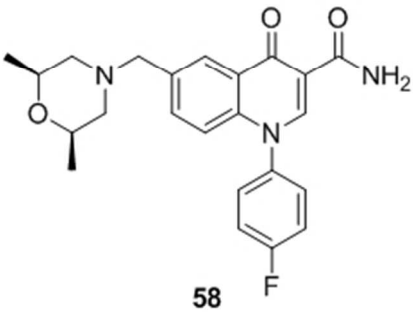

58

$mGlu_2$ IC_{50} = 207 nM

$mGlu_3$ IC_{50} > 30 μM

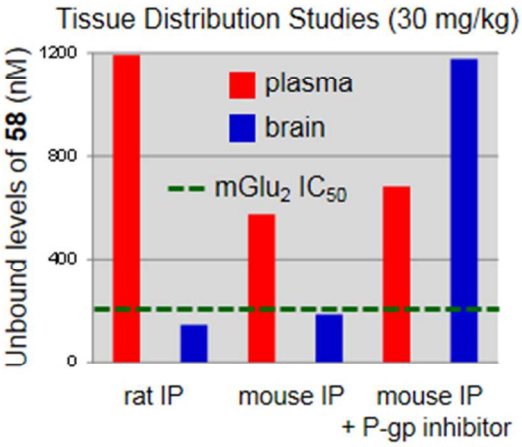

123x58mm (120 x 120 DPI)